

Exceptional service in the national interest



Investigations of Helium Accumulation in Materials through Accelerated Aging

Caitlin A. Taylor

Senior Member of the Technical Staff

Sandia National Laboratories

02/22/18

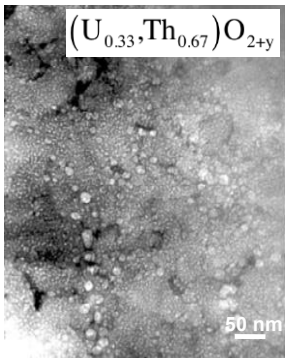
Outline

1. Education and Career
2. He bubble formation in pyrochlores $\text{Gd}_2\text{Ti}_2\text{O}_7$ and $\text{Gd}_2\text{Zr}_2\text{O}_7$
3. Helium diffusion in pyrochlores $\text{Gd}_2\text{Ti}_2\text{O}_7$ and $\text{Gd}_2\text{Zr}_2\text{O}_7$
4. Synergistic effects of damage and gas accumulation in LiAlO_2
5. Helium bubble nucleation and growth in palladium
6. Technical Qualifications

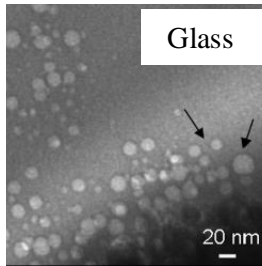
He Bubble Formation in Pyrochlores $\text{Gd}_2\text{Ti}_2\text{O}_7$ and $\text{Gd}_2\text{Zr}_2\text{O}_7$

Crystalline nuclear waste forms

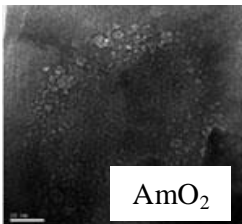
- ❖ Radionuclides are incorporated directly into lattice site positions, increasing the chemical durability (i.e. lower leach rates) of the waste form.
 - Complex crystal structures are required for incorporation of varying radionuclide radii
 - Continuous α -decay of actinides over geological time results in displacement damage and He accumulation
 - He bubbles can lead to cracking and subsequent leaching of radioactive material



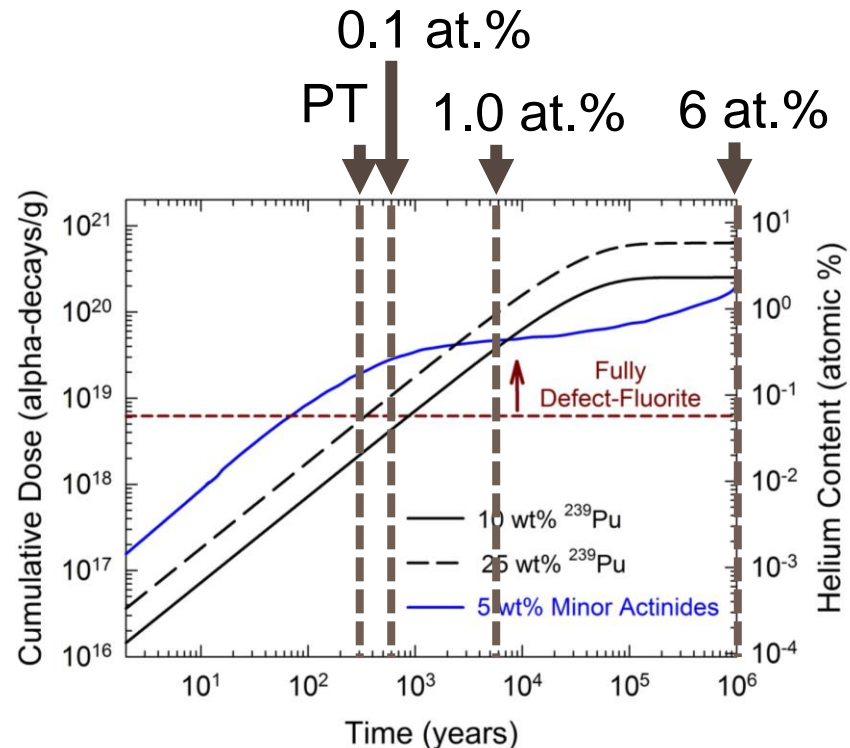
T. Wiss *et al.*, JNM (2014)



G. Gutierrez *et al.*, JNM (2014)

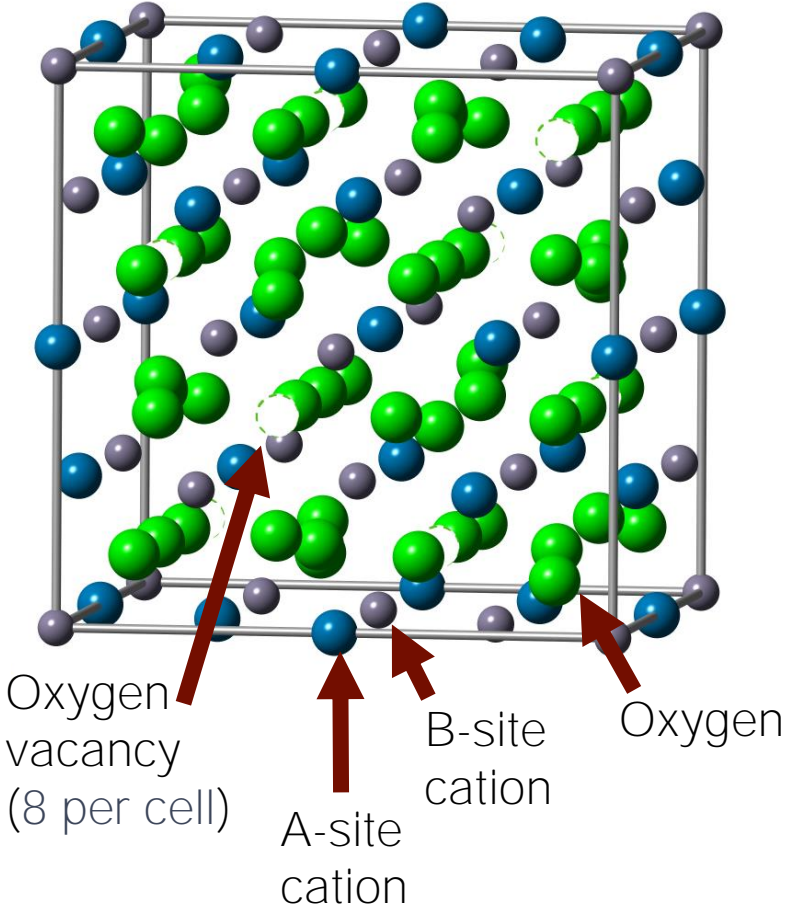


T. Wiss *et al.*, JNM (2015)



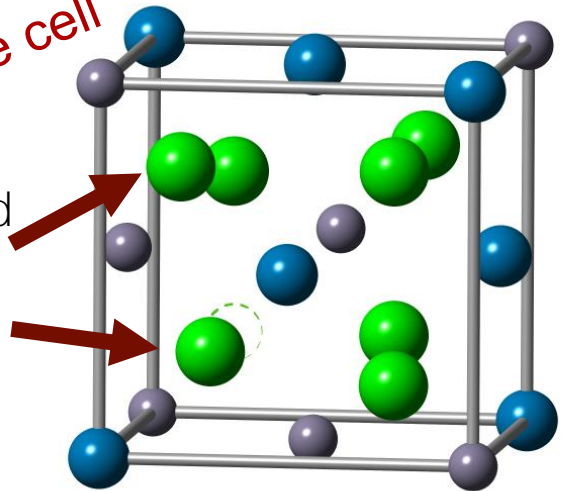
Pyrochlore, $A_2B_2O_7$, is similar to the fluorite crystal structure

Full Pyrochlore Unit Cell



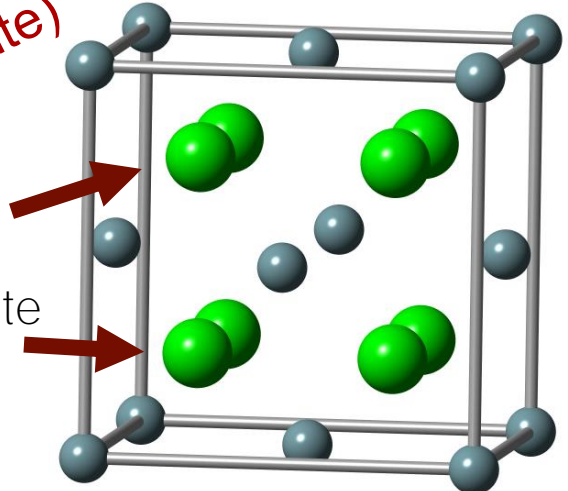
1/8th of pyrochlore cell

Oxygens are shifted from fluorite sites by $48f$ positional parameter



UO₂ (perfect fluorite)

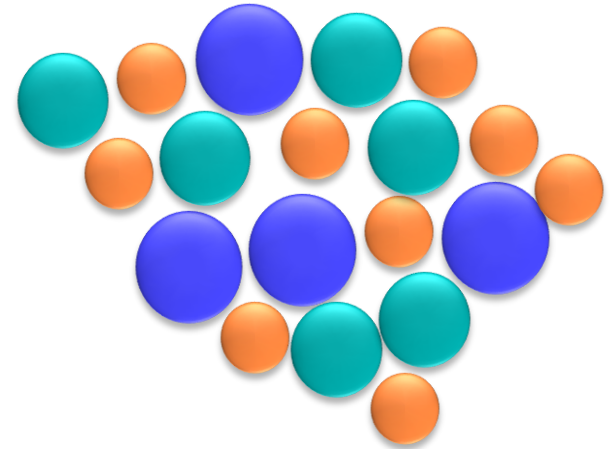
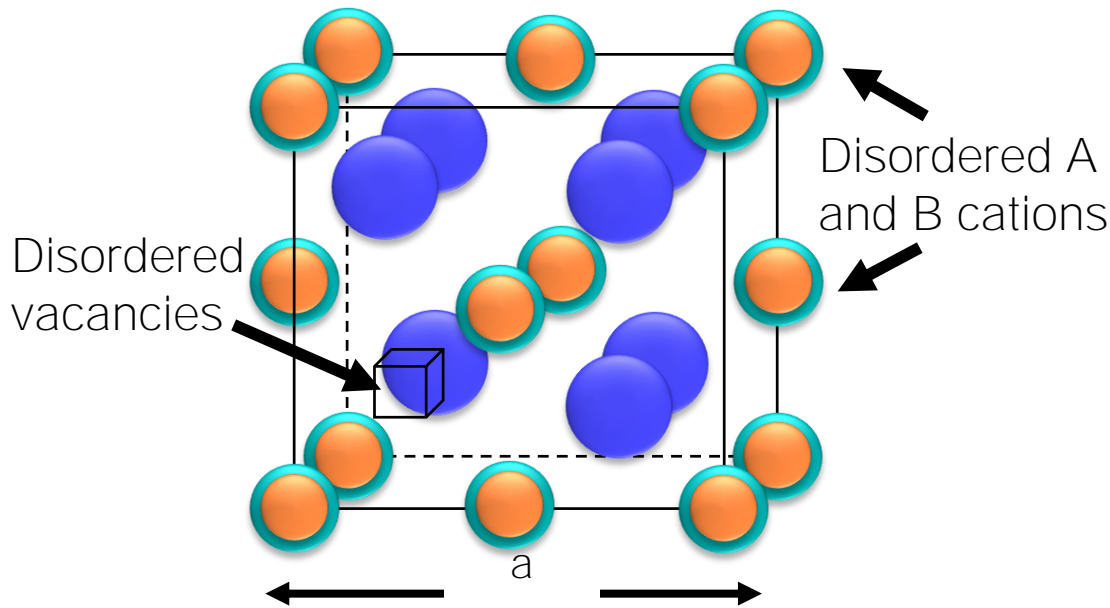
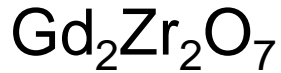
Oxygens on perfect fluorite sites



Pyrochlore behavior under irradiation

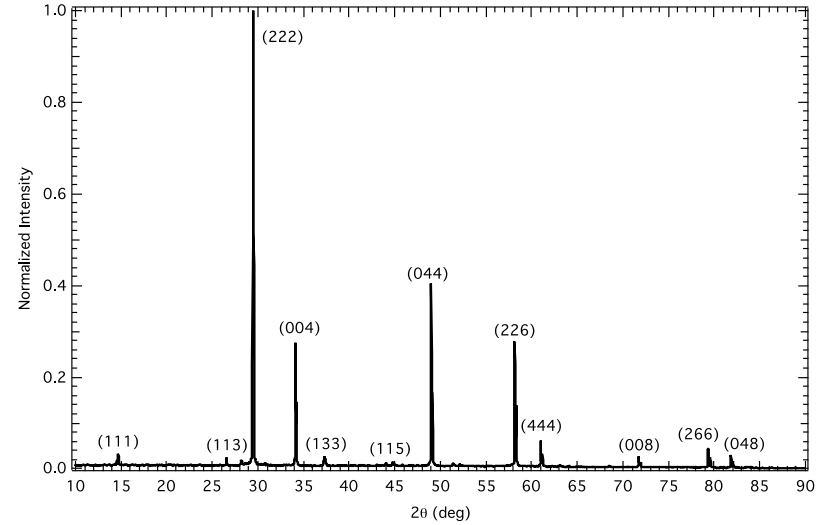
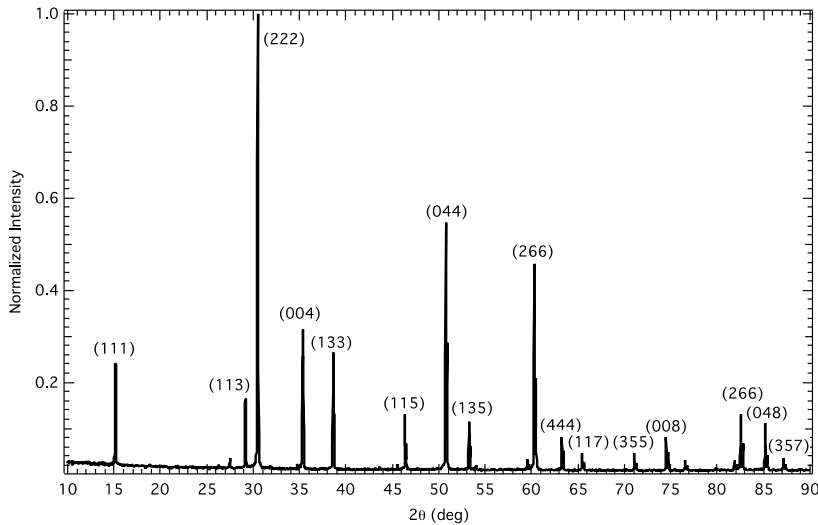
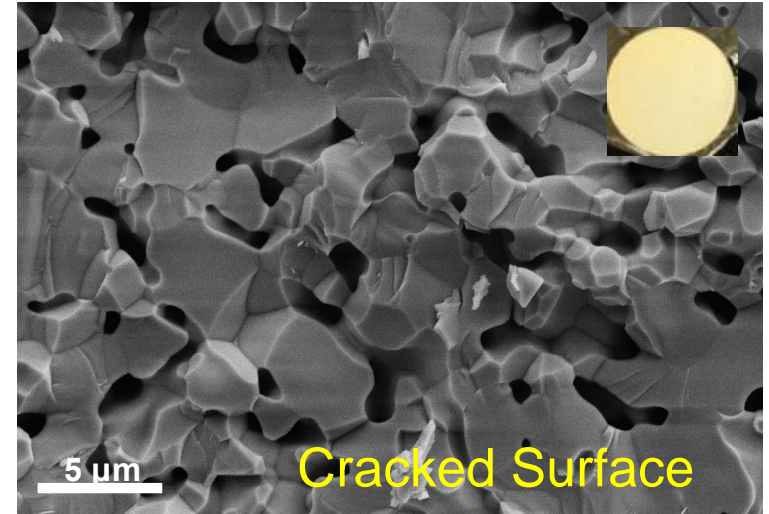
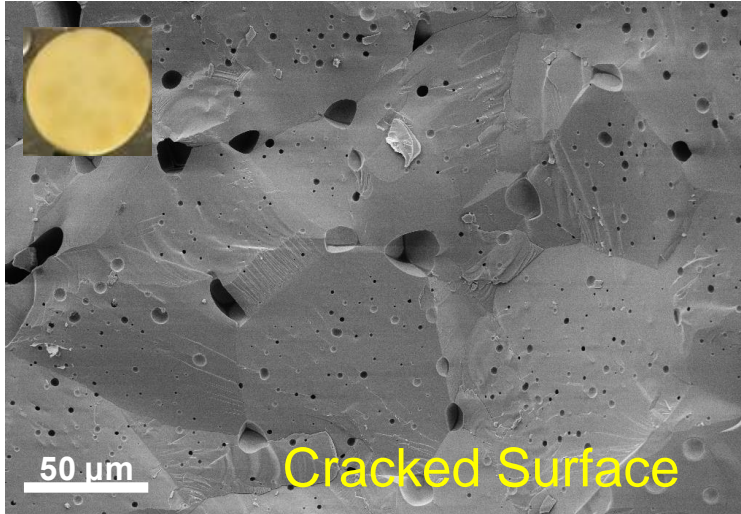
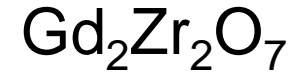
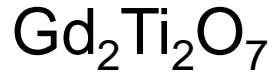
Pyrochlore phase stability depends on A- and B-site cation radius ratio (r_A/r_B)

- We chose to study $Gd_2Ti_2O_7$ and $Gd_2Zr_2O_7$ because they are on opposite ends of the stability range



These transformations would occur prior to any significant He accumulation!

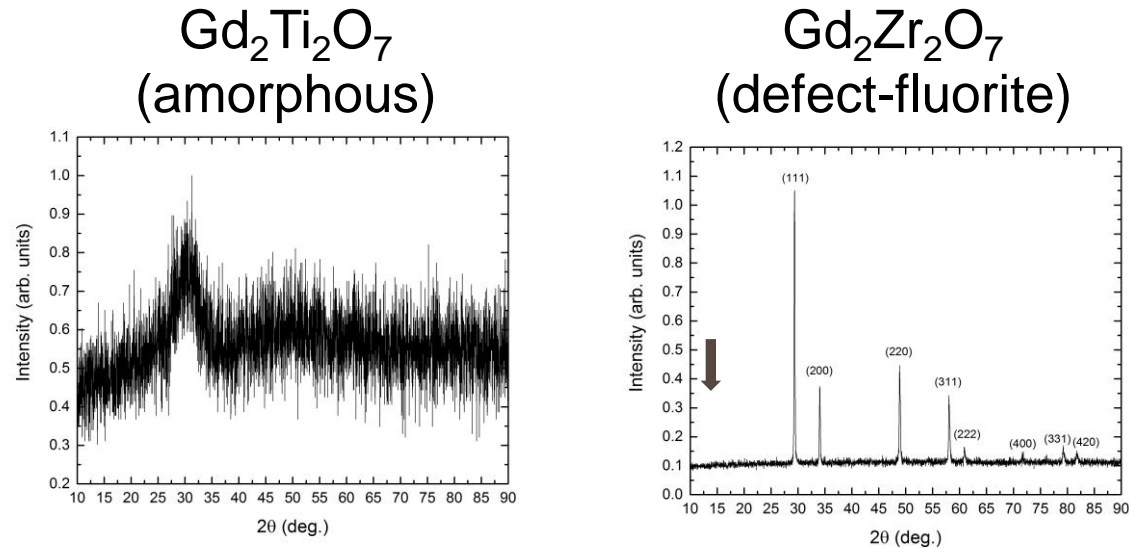
Pyrochlores were synthesized by conventional solid state methods in air



Perfect Single Phase

Samples were ion irradiated to simulate damage and He accumulation expected in waste

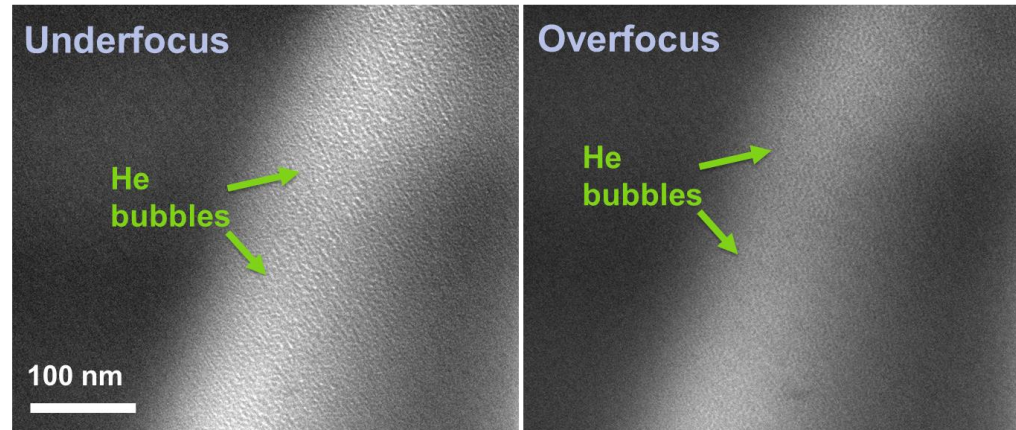
- Irradiation damage and He accumulation were simulated using ion beams
- Samples were pre-damaged with 7 MeV Au³⁺ to a fluence of 2.2×10^{15} Au/cm² (8 dpa at the peak)
- Simulates (1) α -recoil damage, and (2) phase transformations



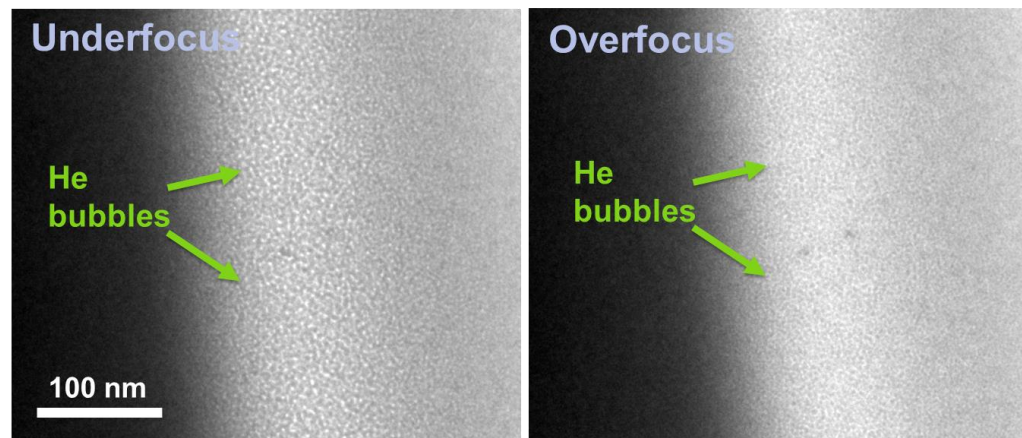
- After pre-damage, samples were implanted with helium:
 - 2×10^{15} He/cm² (0.1 at.% at peak) 200 keV He
 - 2×10^{16} He/cm² (1 at.% at peak) 200 keV He
 - 2×10^{17} He/cm² (12 at.% at peak) 65 keV He

Gd₂Ti₂O₇ formed bubbles after ~6 at% He

- No bubbles were observed in pre-damaged (amorphous) He implanted Gd₂Ti₂O₇ at up to 2×10^{16} He/cm² (1 at.% at peak) He.
- Bubbles were finally observed in the pre-damaged sample implanted with 2×10^{17} He/cm²



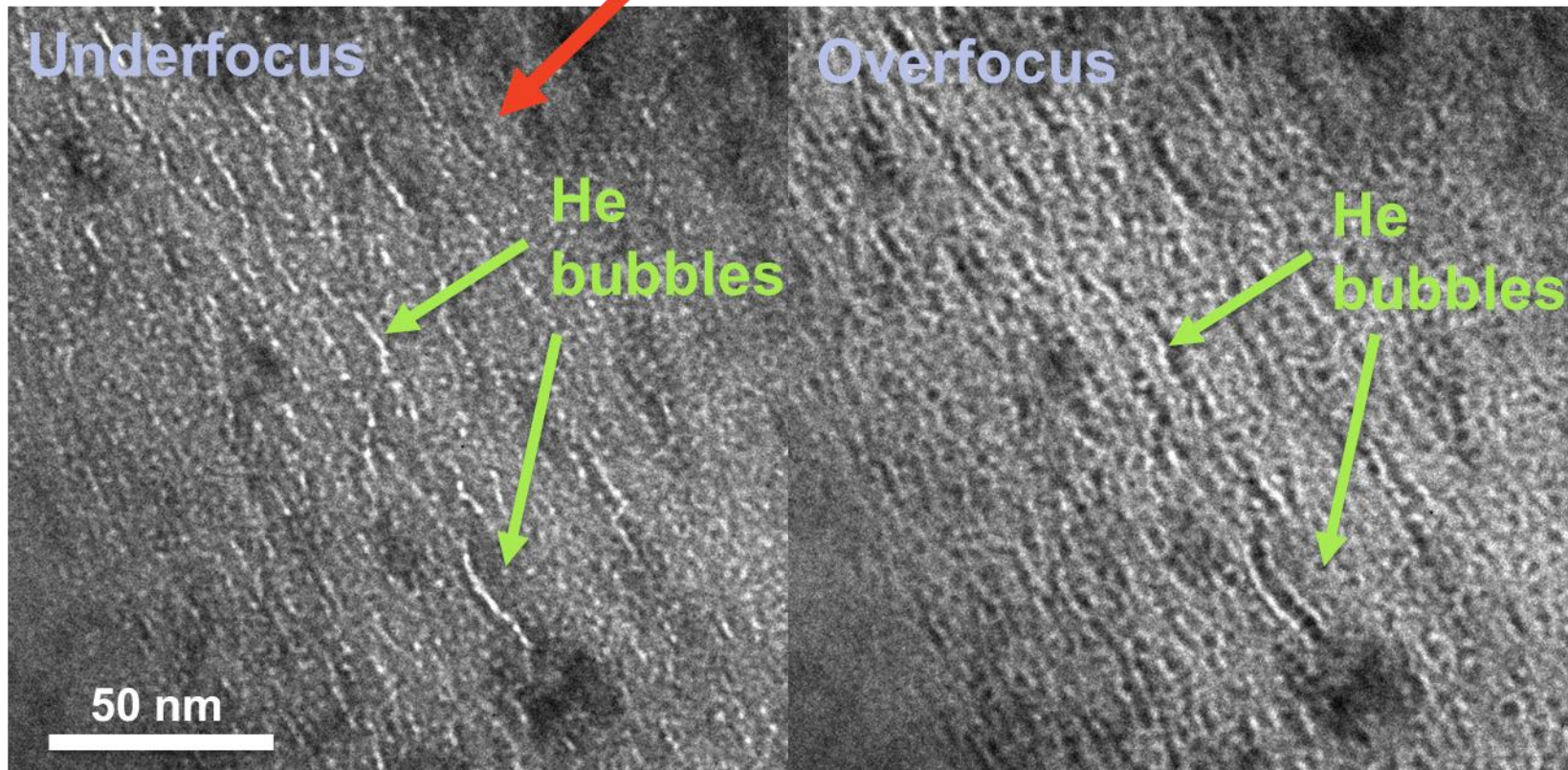
- Bubbles were also observed in pristine (unirradiated) Gd₂Ti₂O₇ implanted with 2×10^{17} He/cm²



$\text{Gd}_2\text{Zr}_2\text{O}_7$ formed bubbles after ~ 4.6 at.% He

- No bubbles were observed in samples implanted with up to 2×10^{16} He/cm² (1 at.% at peak)
- Bubbles were observed in sample implanted with 2×10^{17} He/cm² (12 at.% at peak)

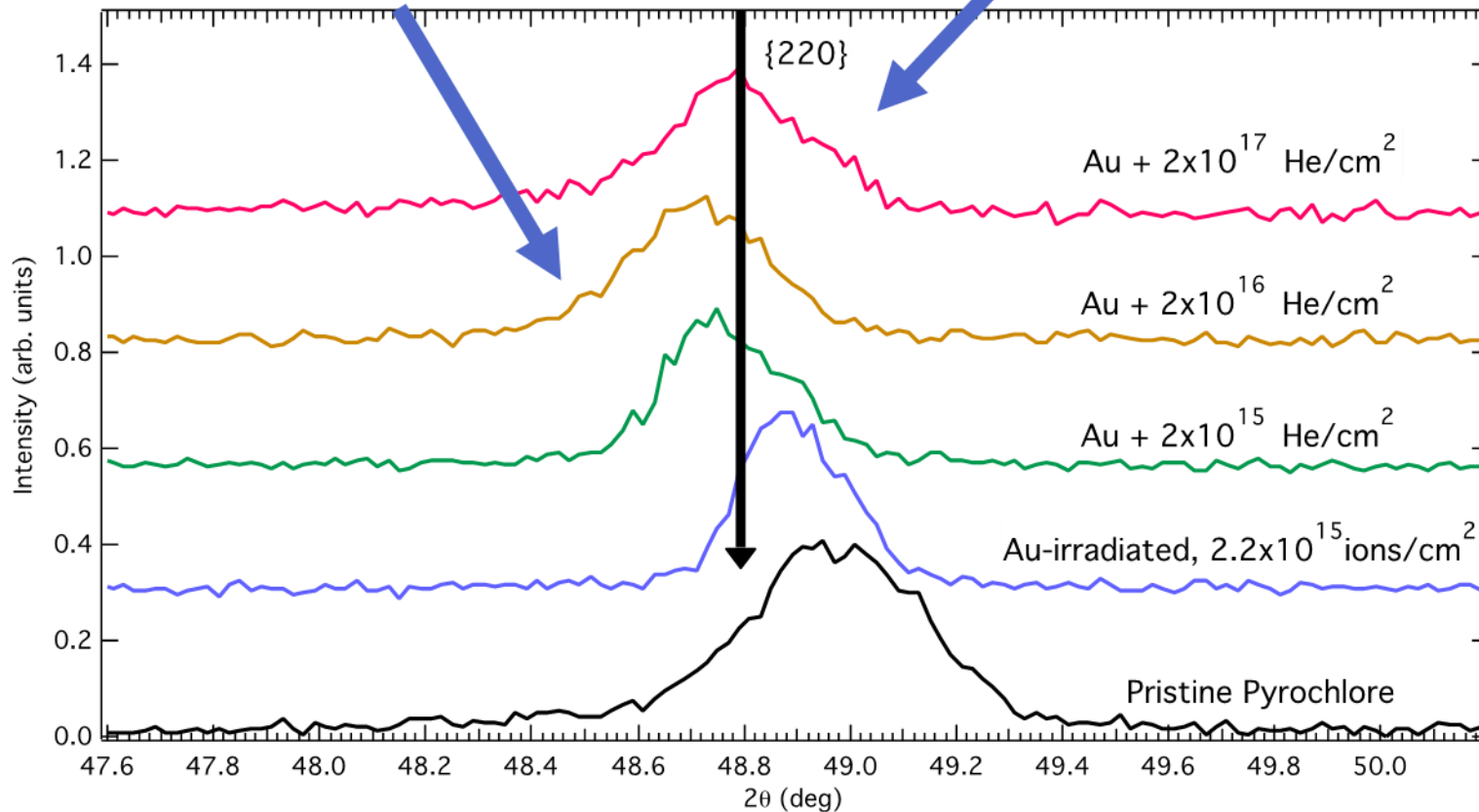
Individual bubbles formed
“chains” 10-30 nm in length



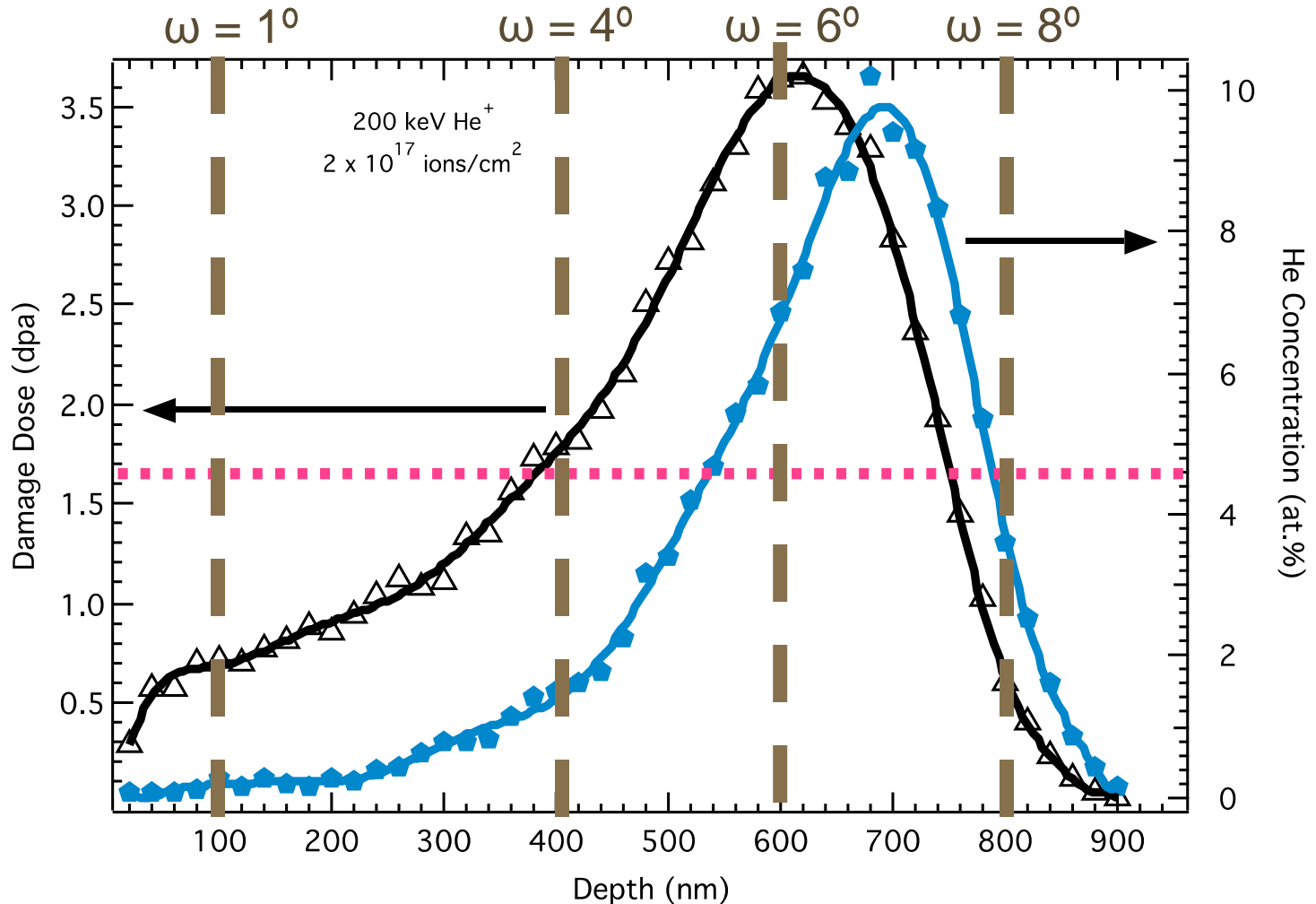
GIXRD measurements showed clear peak shifts in all irradiated $\text{Gd}_2\text{Zr}_2\text{O}_7$ samples

Lattice parameter increased with 2×10^{15} and 2×10^{16} He/cm^2

Lattice parameter decreased with 2×10^{17} He/cm^2 (when bubbles formed)

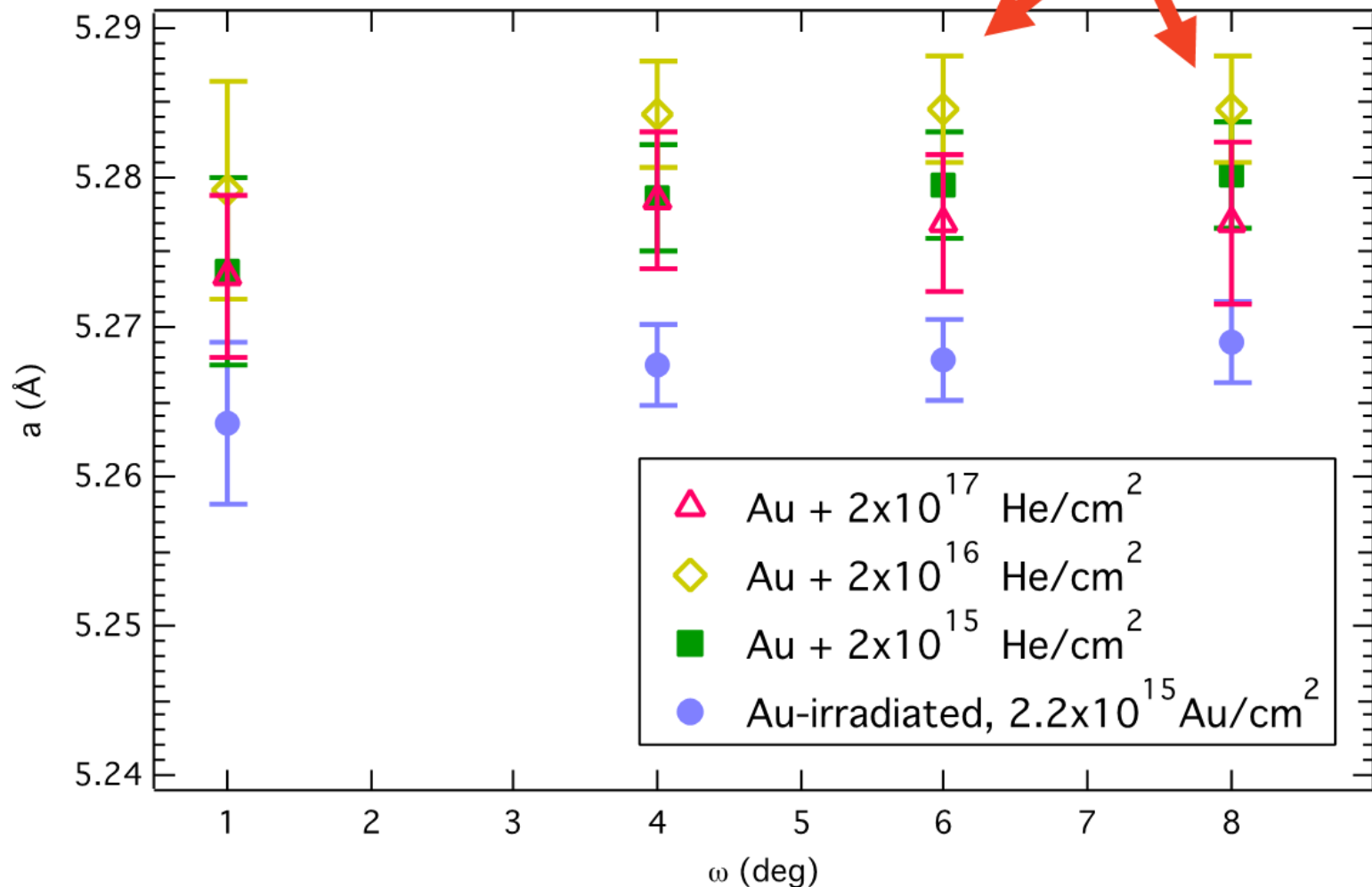


Lattice parameter was calculated using several x-ray penetration depths



Lattice parameter decreases when He bubbles form in defect-fluorite $\text{Gd}_2\text{Zr}_2\text{O}_7$

X-rays probe depth where bubbles were first observed



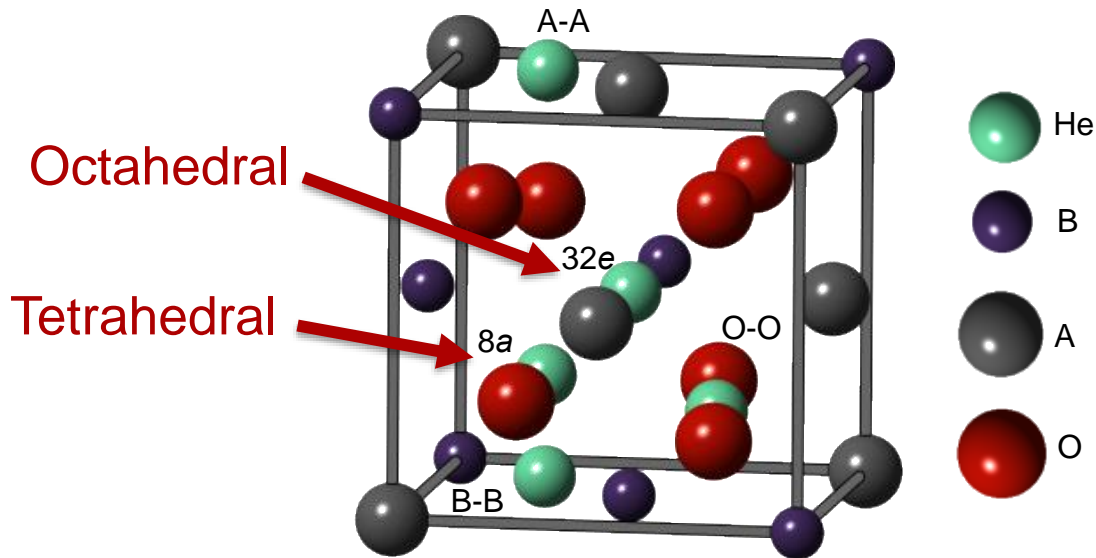
He Diffusion in Pyrochlores $\text{Gd}_2\text{Ti}_2\text{O}_7$ and $\text{Gd}_2\text{Zr}_2\text{O}_7$

In a perfect lattice, He resides in interstitial sites

He was shown to prefer the octahedral interstitial site in $Y_2Ti_2O_7$, prefers individual sites as opposed to clustering

→ did not consider vacancy binding

- Danielson *et al.* JNM 452 (2014) 189-196.
- Yang *et al.* JAP 115 (2014) 143508.



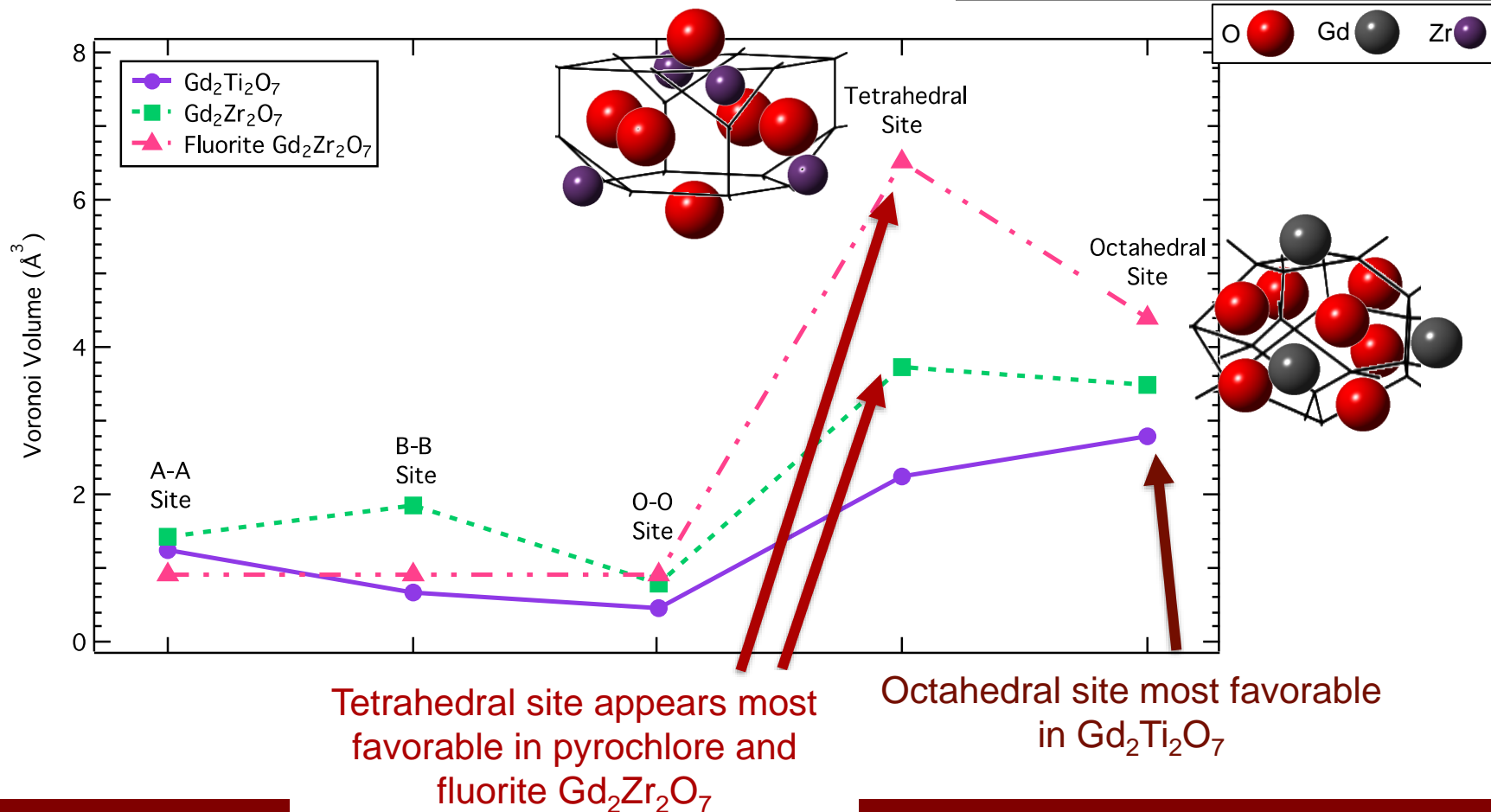
Interstitial He diffuses between octahedral sites with $E_m \sim 0.5$ eV in $Y_2Ti_2O_7$

- Danielson *et al.* JNM 477 (2016) 215-221.

Preferred site for interstitial He can be predicted using Voronoi volume calculations

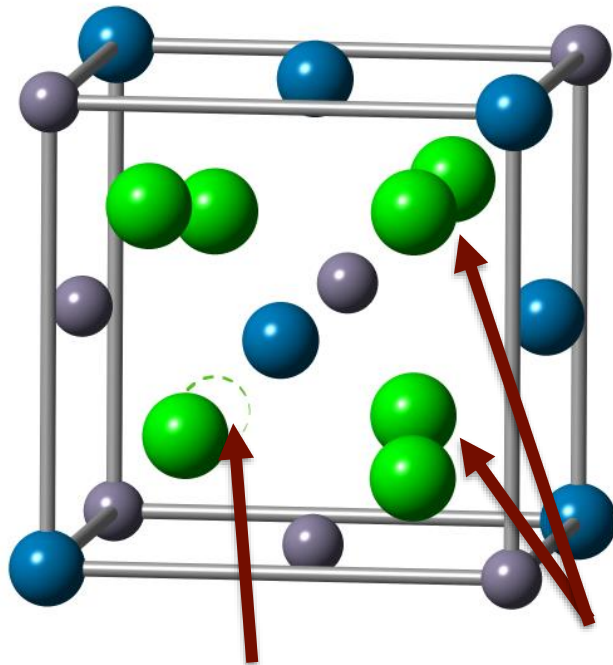
- Lowest energy interstitial He site is typically directly related to the Voronoi volume of the interstitial site in oxides
 - Erhart JAP 111 (2012) 113502.

Voronoi volumes calculated using Voro++ C++ library



In pyrochlores, oxygen atom positions influence site volume and therefore He binding energy

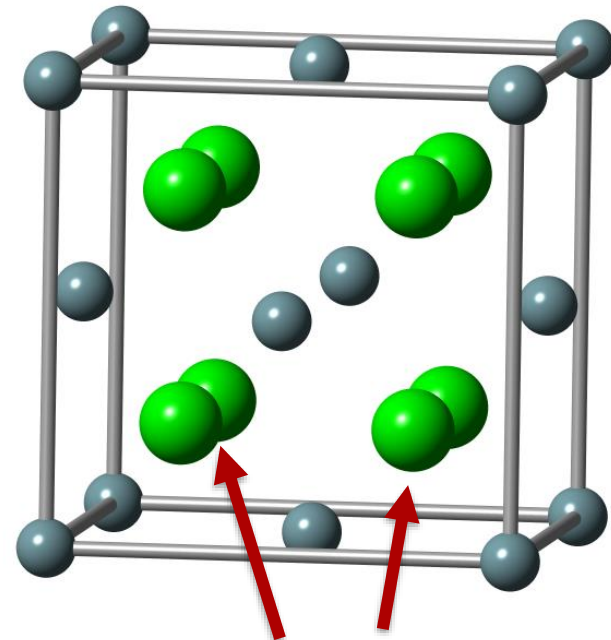
1/8th of Pyrochlore
Unit Cell



Structural O
vacancy

O atoms shifted
from fluorite sites

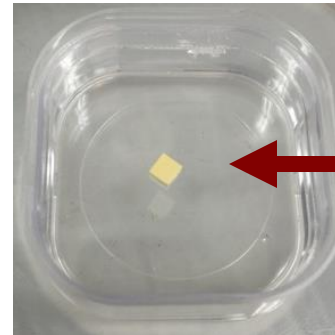
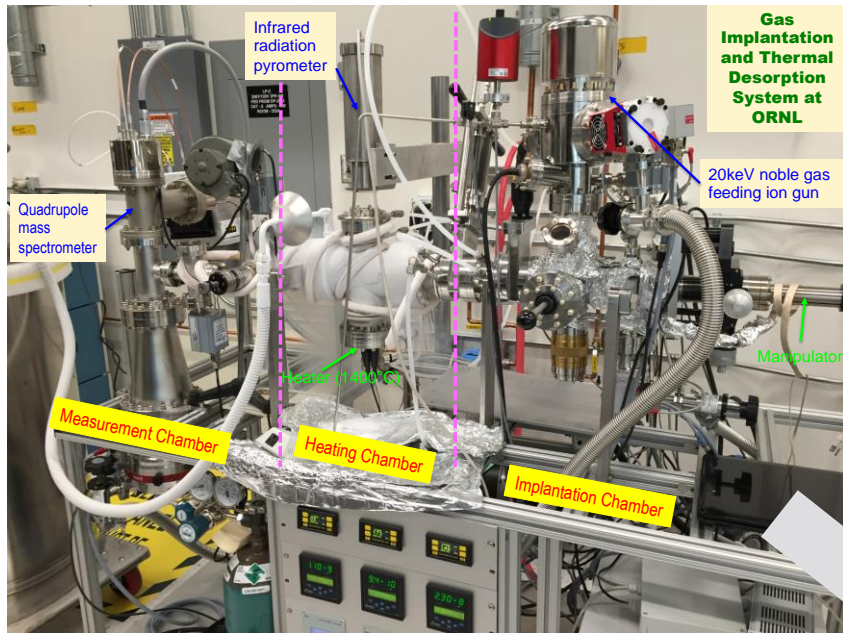
UO₂



O atoms perfectly
positioned on
fluorite sites

B-site cation radius had little effect on the Voronoi volume .

Thermal desorption spectroscopy was used to study He trapping in $Gd_2Ti_2O_7$ and $Gd_2Zr_2O_7$



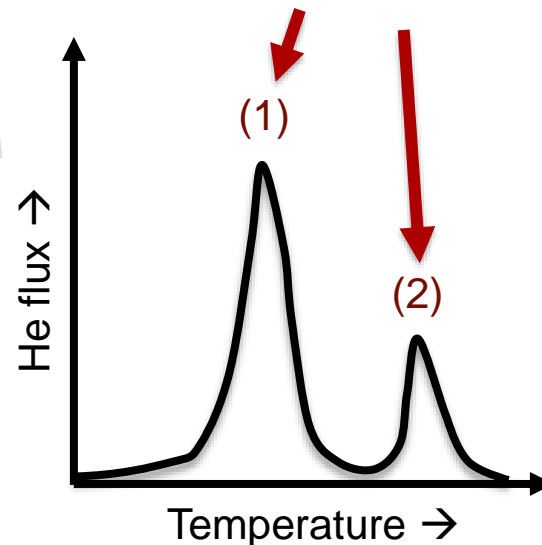
← THDS sample

Each peak corresponds to He dissociation from a different trapping site

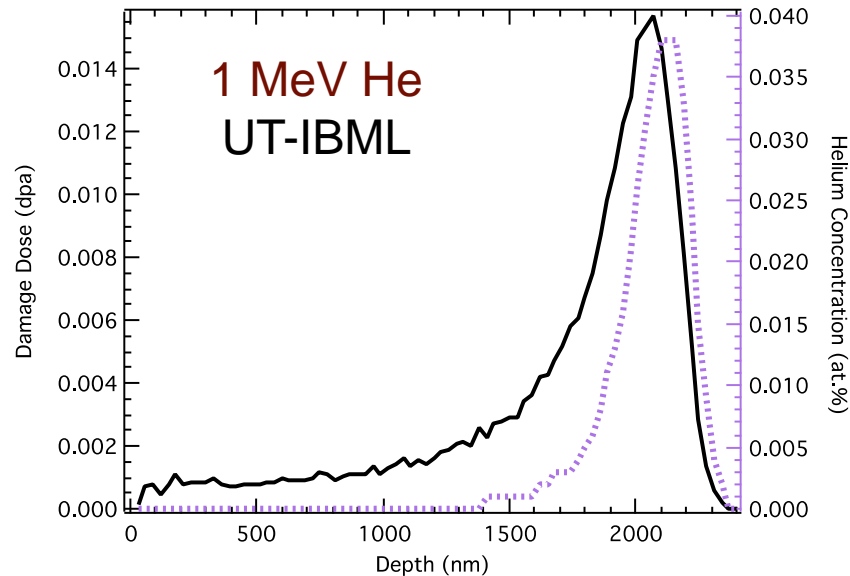
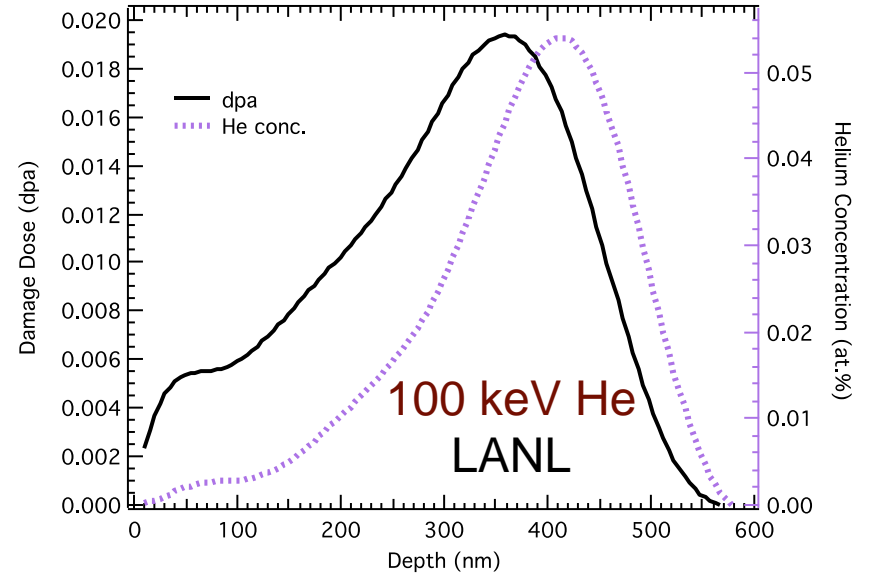
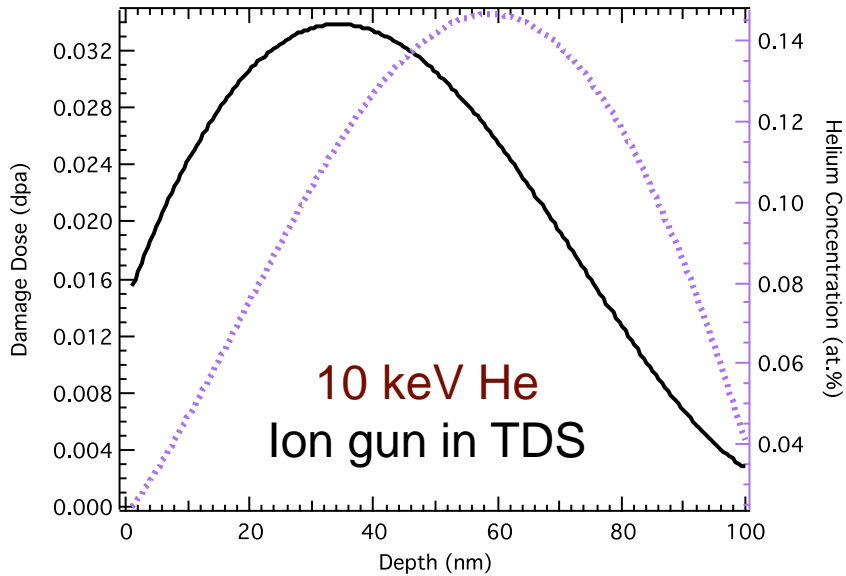
THDS measurements were performed by Xunxiang Hu at Oak Ridge National Laboratory

$$\ln(R/T_m^2) = -E_D/k_B T_m + \ln(\nu k_B/E_D)$$

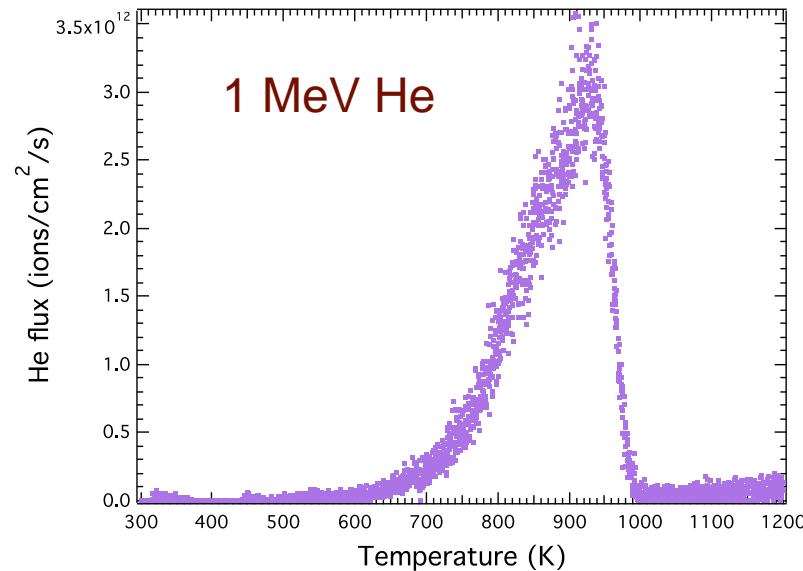
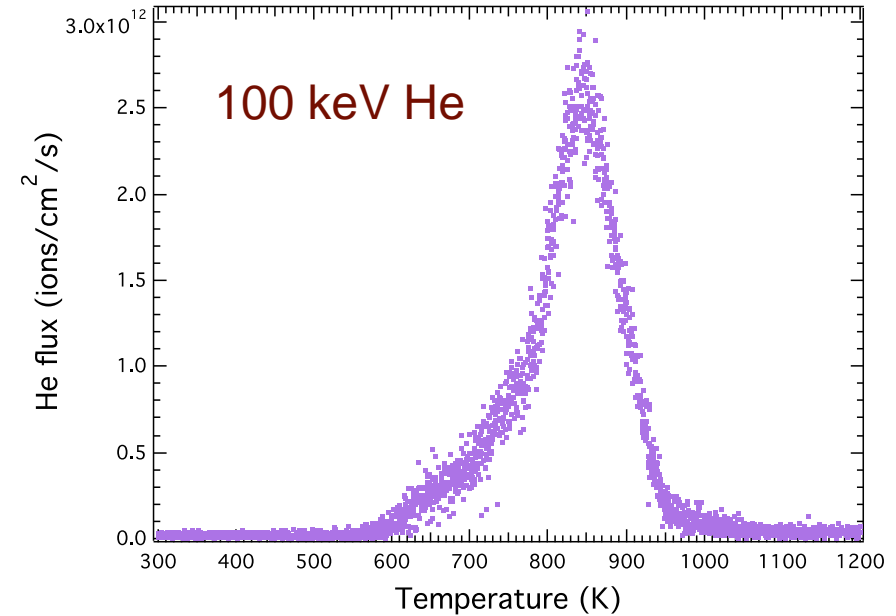
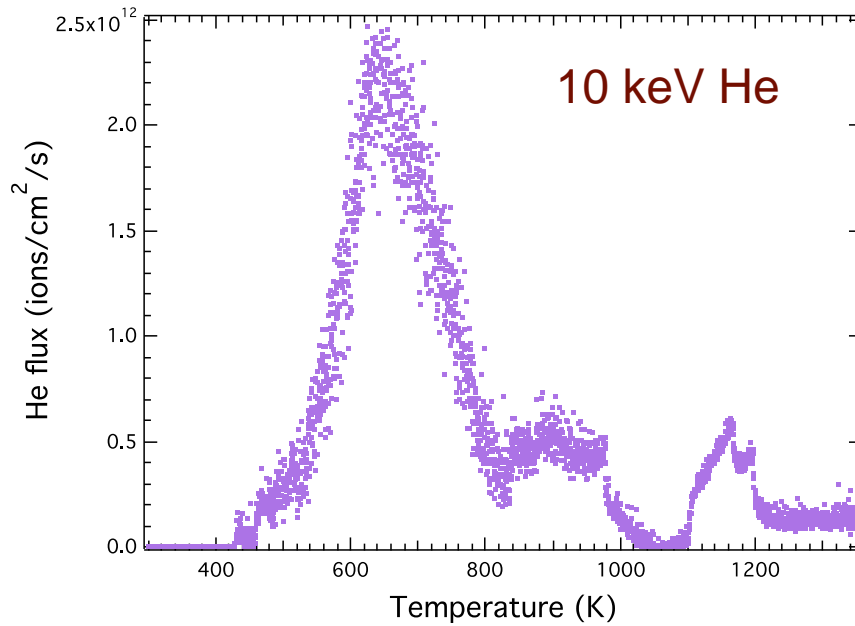
$$E_D = E_m + E_B$$



Samples were implanted at 3 different energies



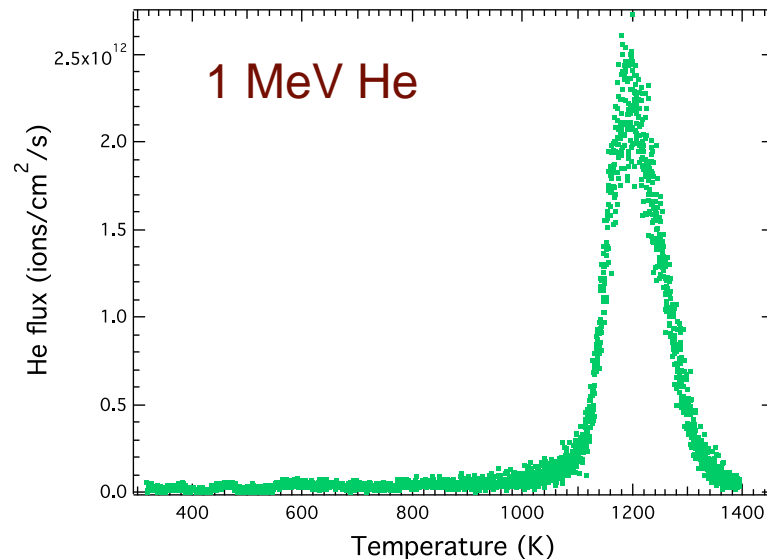
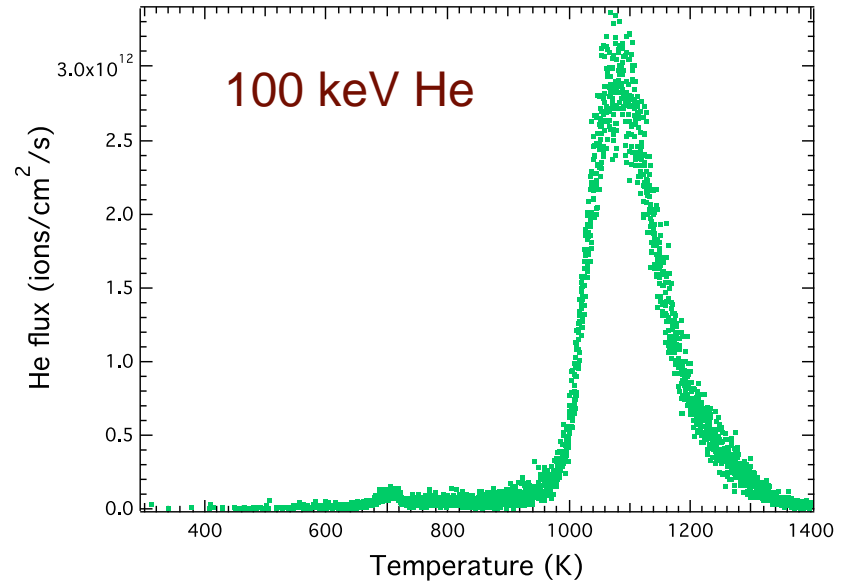
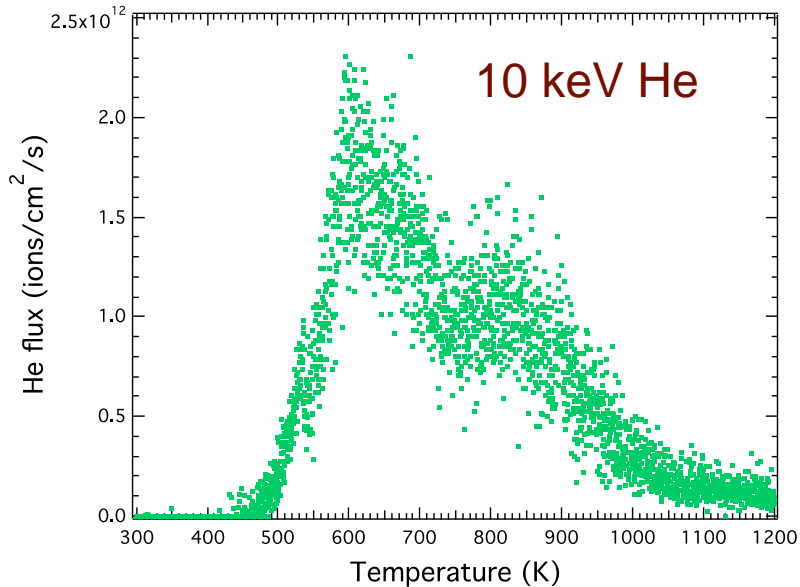
Desorption profiles differed for each implantation energy in $\text{Gd}_2\text{Zr}_2\text{O}_7$



Profiles are fit with overlapping peaks using fitting software

100 keV and 1 MeV peaks are shifted to a *slightly* higher T

Desorption peaks occurred at much higher temperatures in high energy implanted $Gd_2Ti_2O_7$



100 keV and 1 MeV peaks are much higher T than $Gd_2Zr_2O_7$!

Dissociation energies were calculated based on peak desorption temperatures

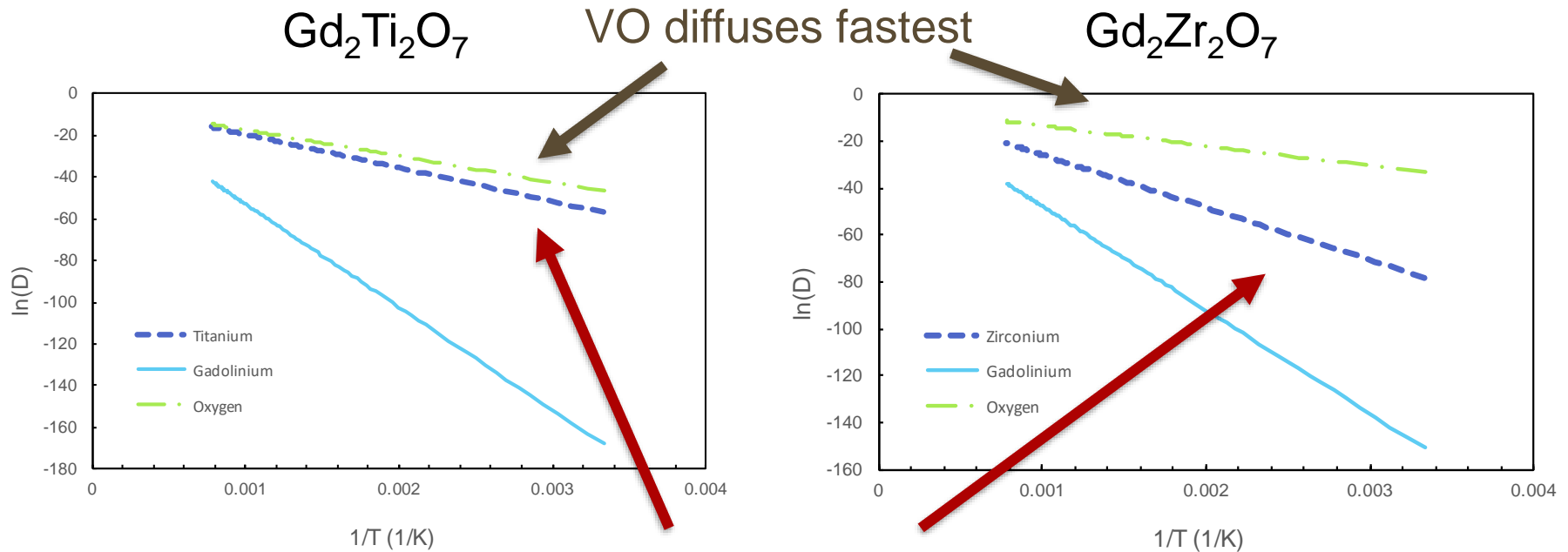
		$\text{Gd}_2 \text{Ti}_2 \text{O}_7$		$\text{Gd}_2 \text{Zr}_2 \text{O}_7$	
		T_m (K)	E_D (eV)	T_m (K)	E_D (eV)
10 keV	Peak 1	615	1.77	656	1.90
	Peak 2	796	2.32	800	2.33
100 keV	Peak 1	1058	3.11	794	2.31
	Peak 2	1107	3.25	850	2.48
1 MeV	Peak 1	1179	3.47	860	2.51
	Peak 2	1213	3.57	931	2.72

- **10 keV** dissociation energies are very similar and likely **single vacancies**
 - ~ 800 K likely VGd, 615 K likely VTi, and 656 K likely VZr
- **100 keV, 1 MeV** dissociation energies are higher for both pyrochlores
 - Higher energies probably due to He binding to **vacancy clusters**
 - Vacancy clusters could form during the heating or during irradiation

He could re-trap in vacancy clusters that form during the heating, below 800 K

Vacancy diffusivity was estimated using literature values for E_m^v

$$D = D_o e^{-E_m/kT} \quad D_o = \frac{1}{6} \lambda^2 f z v e^{\Delta S_m/k}$$

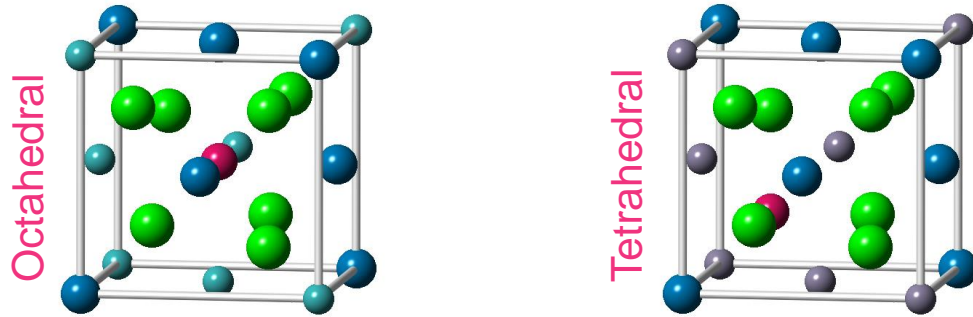


V_{Ti} is mobile at 500 K, V_{Zr} is mobile at 700 K

Oxygen vacancies have highest mobility in both materials, but may be more likely to recombine

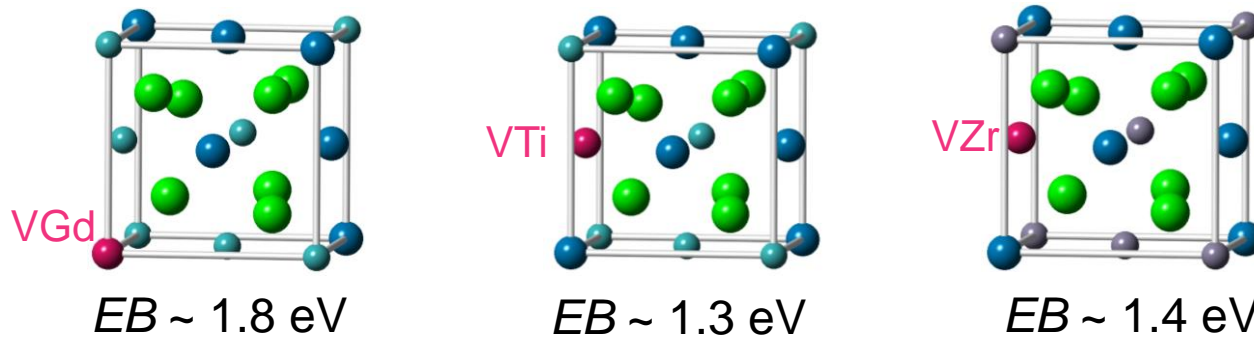
Summary of He migration in Gd₂Ti₂O₇ and Gd₂Zr₂O₇

In a perfect lattice, interstitial He will reside in the octahedral site in Gd₂Ti₂O₇ and the tetrahedral site in pyrochlore or defect-fluorite Gd₂Zr₂O₇



He probably binds to single vacancy sites in a damaged pyrochlore at 300 K

- Likely cation vacancies because there are only two TDS peaks



Need to confirm with DFT

At high temperatures, He binds to vacancy clusters

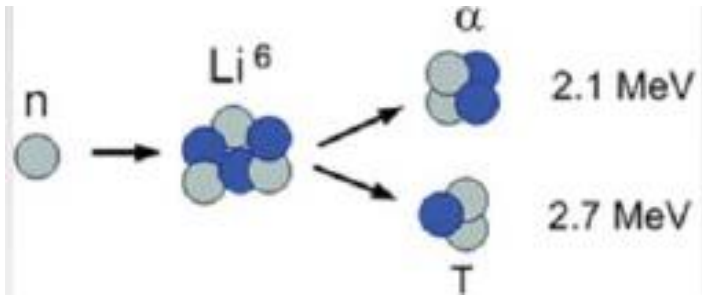
VGd are immobile, VO are highly mobile

VTi is more mobile than VZr → larger vacancy clusters expected in Gd₂Ti₂O₇

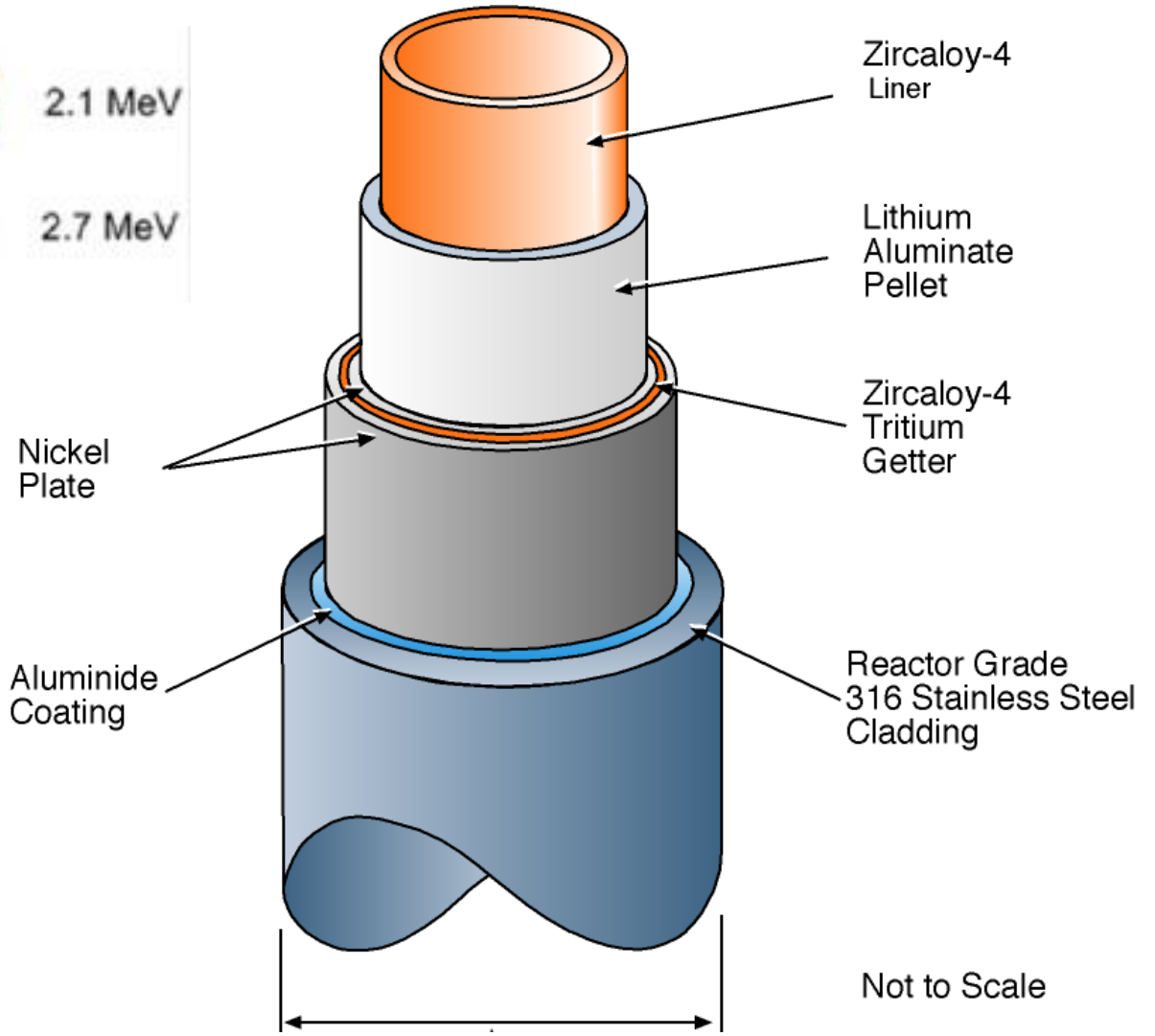
Vacancies have very low mobility at 300 K over geological time (1,000,000 years)

Synergistic Effects of Damage and Gas Accumulation in LiAlO_2

Tritium Producing Burnable Absorber Rod

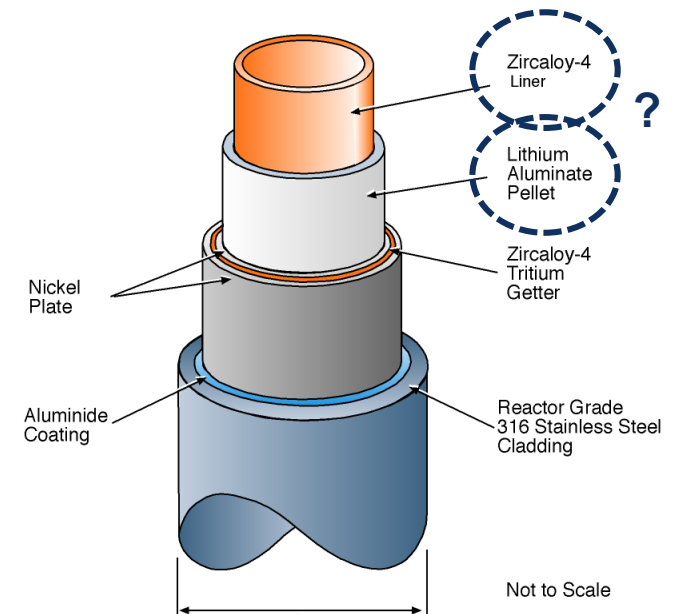
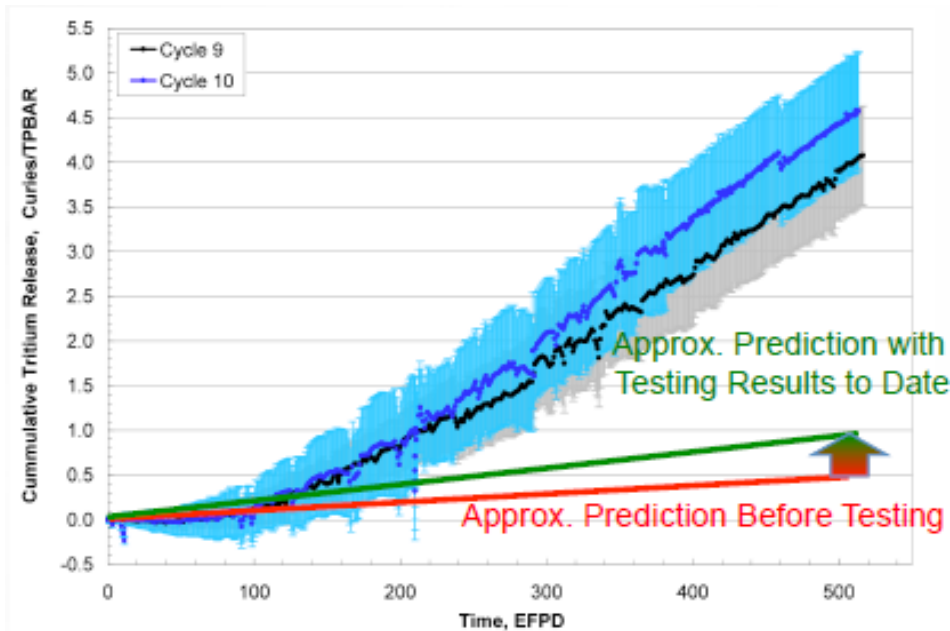


- Displacement Damage
- Helium Implantation
- Tritium Implantation
- Elevated Temperatures



Understanding Tritium Permeation in TPBAR

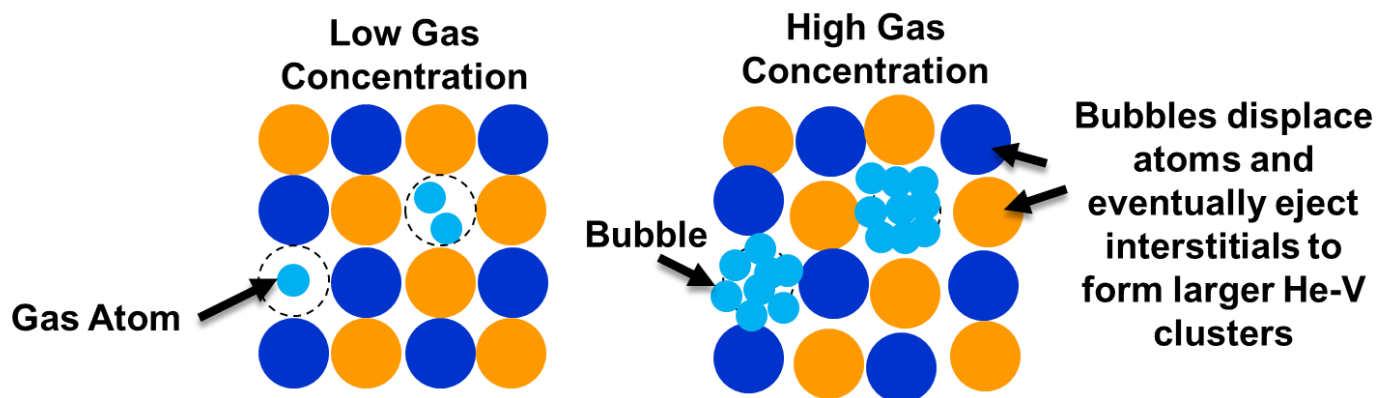
- TPBAR ^3H permeation is higher than predictive performance models
 - In 2004, during Cycle 6, the predicted levels were ~ 0.5 Ci/TPBAR/cycle and actual levels were ~ 4 Ci/TPBAR/cycle (0.04% of total ^3H produced)
- Mechanisms responsible for differences between predictions and observations are not well understood
- Currently building an understanding of fundamental ^3H -He-defect interactions



Burkes, Senor, Longoni and Johns, TFG Meeting
2016, Rochester, NY

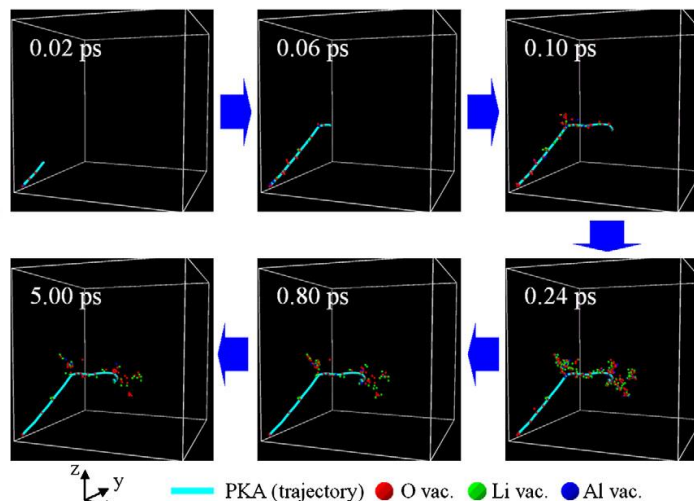
Bubbles May Affect ^3H Release

- ❖ Bubbles form due to He trapping in lattice defects



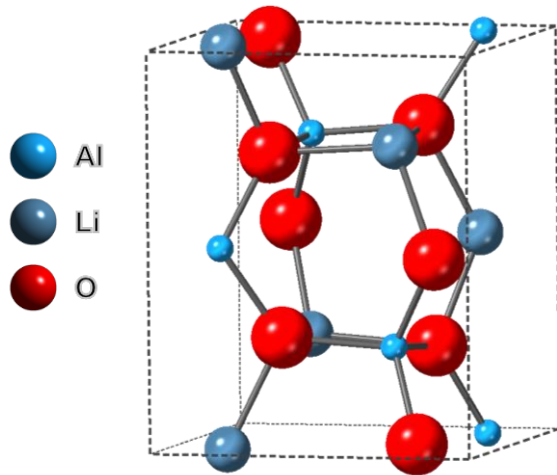
- ❖ Neutron irradiation produces displacement cascades, providing complex defect structures for He or ^3H to trap in.

MD simulation of displacement cascade in LiAlO_2 (PKA = 5 keV)



Tsuchihira *et al* JNM 414 (2011) 44-52

LiAlO₂ Background

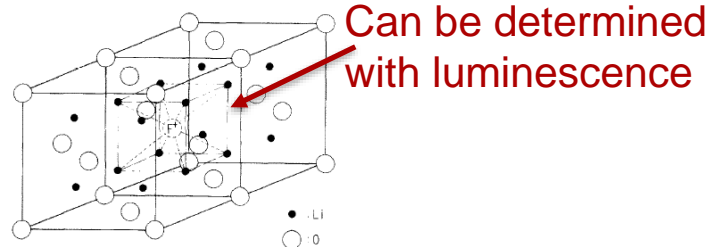


γ -LiAlO₂ is tetragonal
(space group: P 41 21 2)

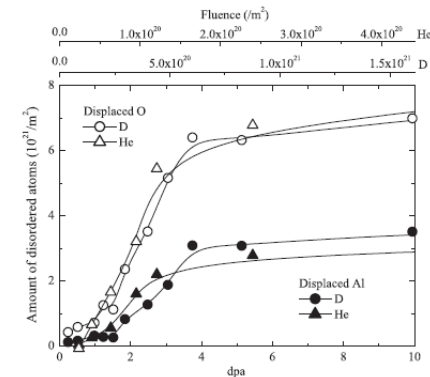
Previous Work

- Structural defects
 - Luo *et al* JNM 372 (2008) 53-58
- Volume swelling
 - Noda JNM 179-181 (1991) 37-41
- ³H detrapping
 - Oyaidzu *et al* JNM 375 (2008) 1-7
- Gas diffusion and release
 - Raffray *et al* JNM 210 (1994) 143-160

- H isotopes are thought to trap in oxygen vacancies
 - ²H release occurs at the same temperature as defect annealing in implanted LiAlO₂



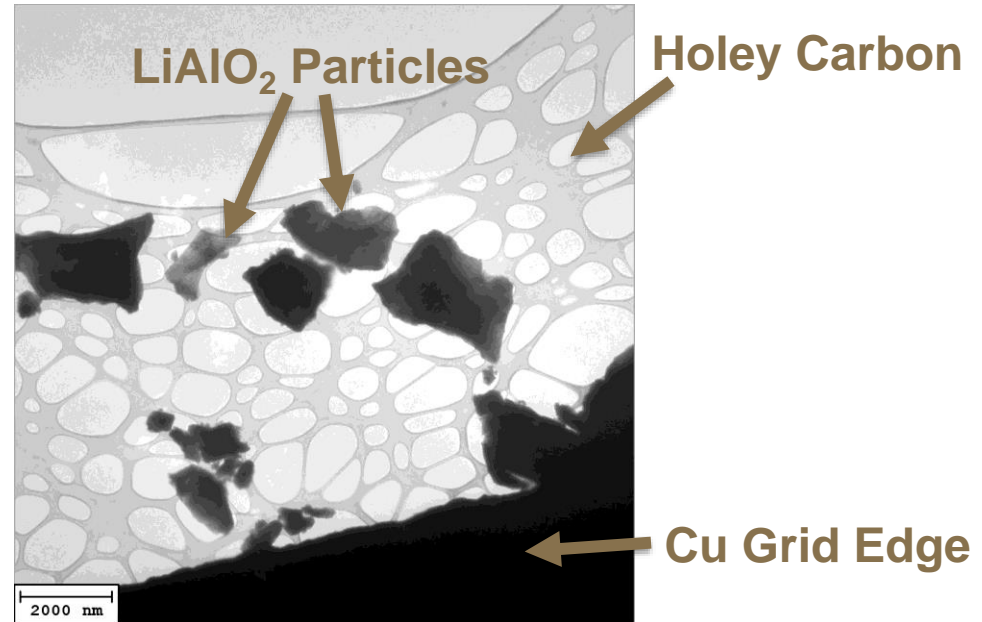
Noda JNM 179-181 (1991) 37-41



29

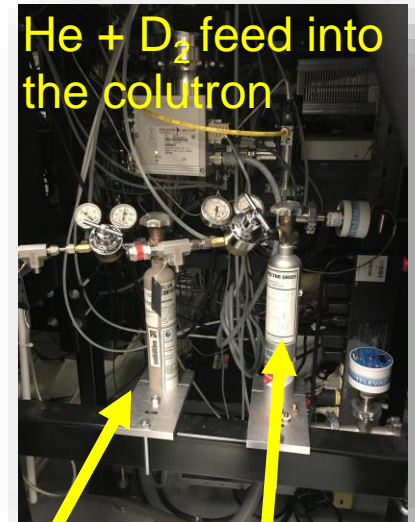
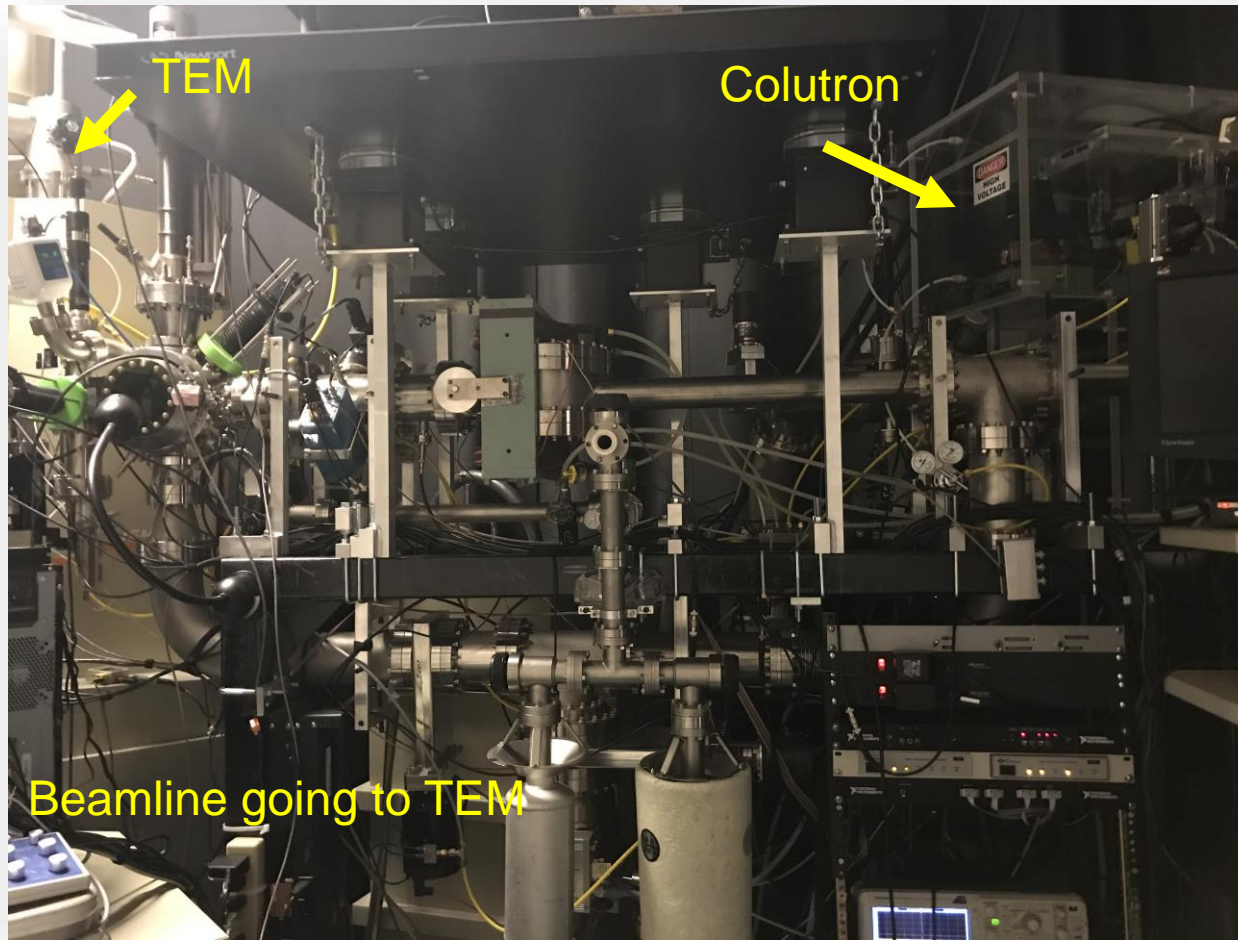
LiAlO₂ in-situ ion irradiation parameters

- ❖ Powders were drop-cast onto TEM grids



- ❖ Samples were heated to **310°C** using Hummingbird HT stage
- ❖ Three sets of irradiations:
 - 10 keV He → simulates He accumulation from ⁶Li transmutation and ³H decay
 - 10 keV He + 5 keV D → simulates He and ³H interaction
 - 10 keV He + 5 keV D + **1.7 MeV Au** → simulates gas build-up + displacement cascades

Sandia's I³TEM in-situ ion irradiation facility



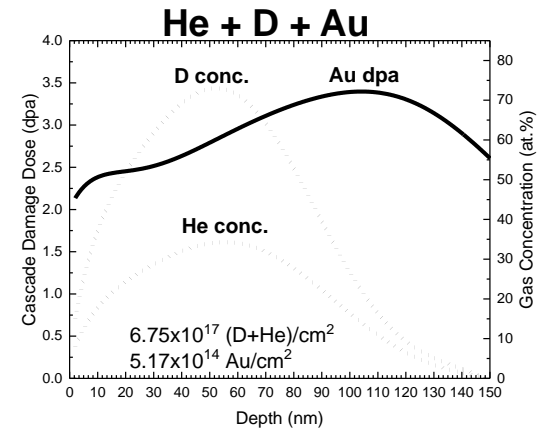
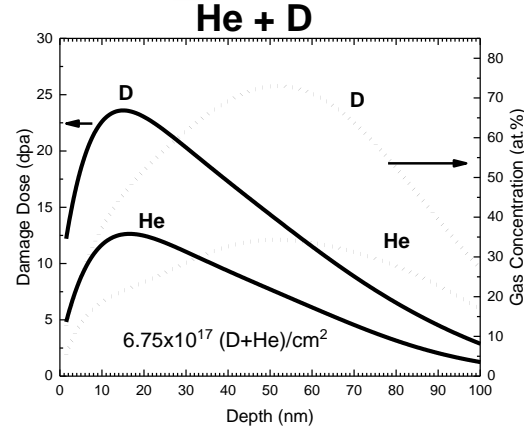
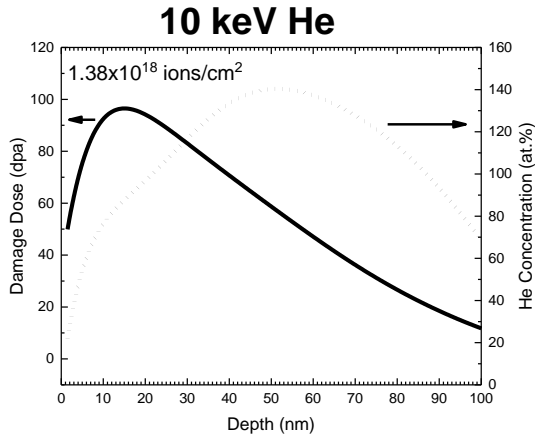
He bottle D₂ bottle

- JEOL 2100 TEM. Samples are tilted to +30° in x to face the ion beam
- Both He and D ions are part of the same ion beam (He + D₂), heavy ions from 6 MV tandem accelerator.

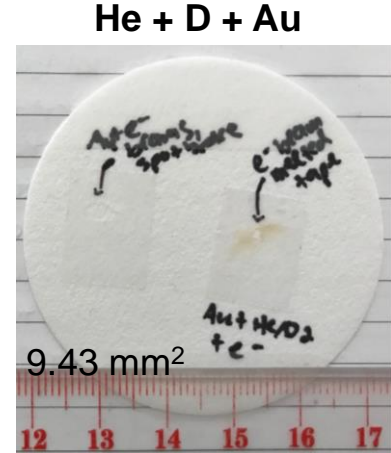
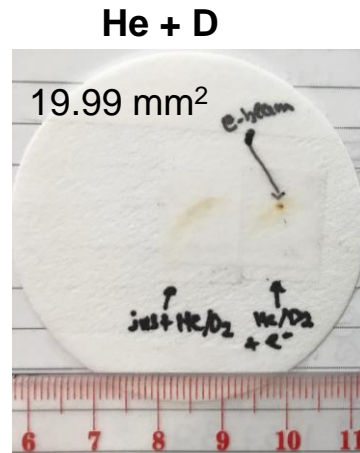
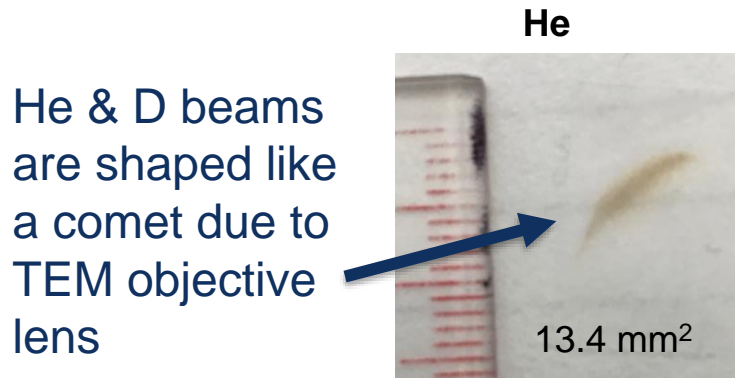
LiAlO₂ in-situ ion irradiation parameters

Most He/D diffuses out of thin film immediately

- SRIM Calculations

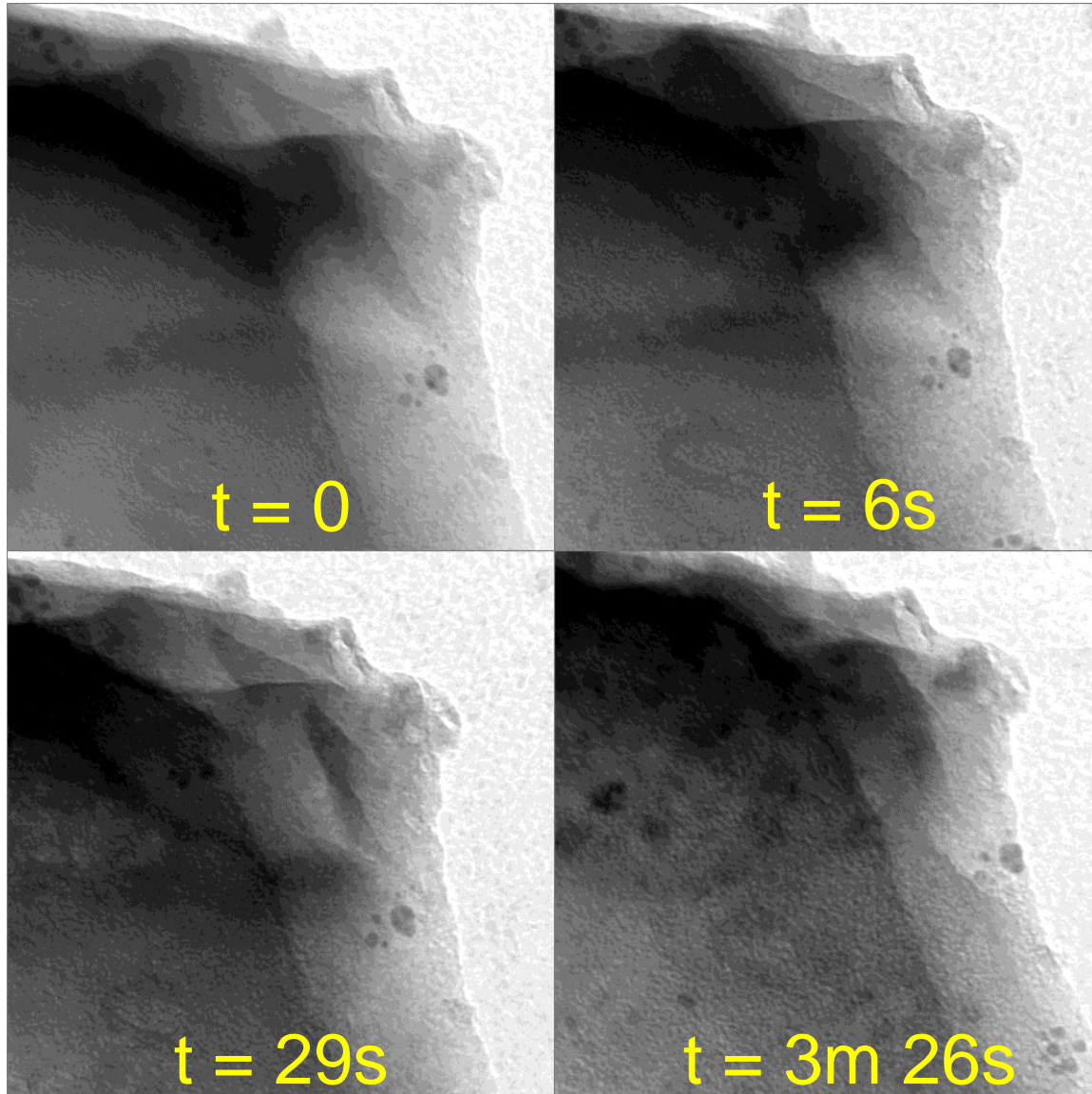
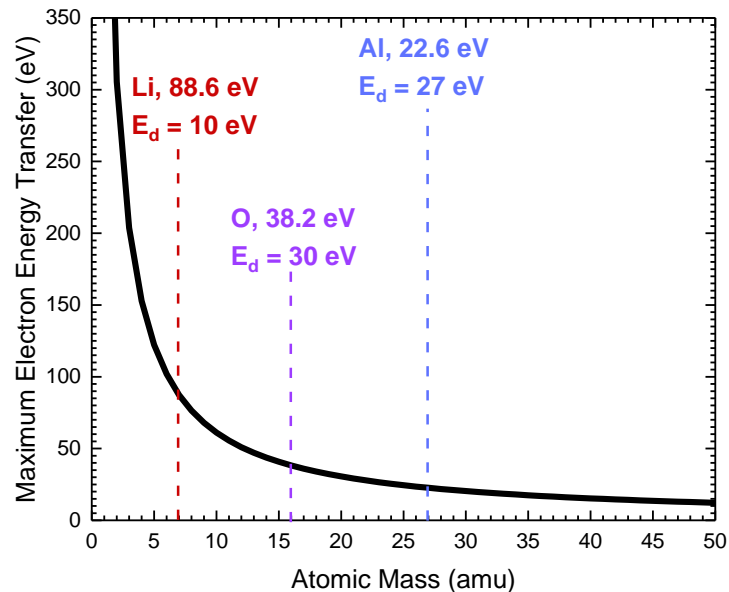


- Burn spots were used (1) to confirm that electron beam spot overlaps ion beam spot and (2) to determine the ion beam irradiation area.



Electron beam induced void growth

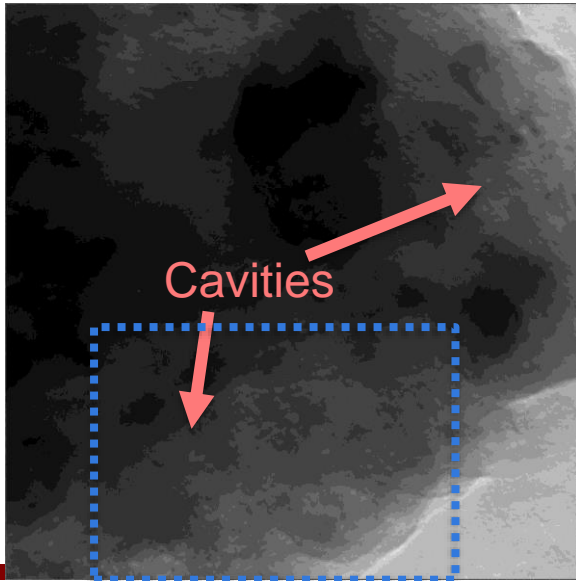
- ❖ Voids were observed to form under the electron beam in several particles
- ❖ Rate of void formation is not consistent between particles
- ❖ Possibly due to electron beam displacing Li and Al atoms



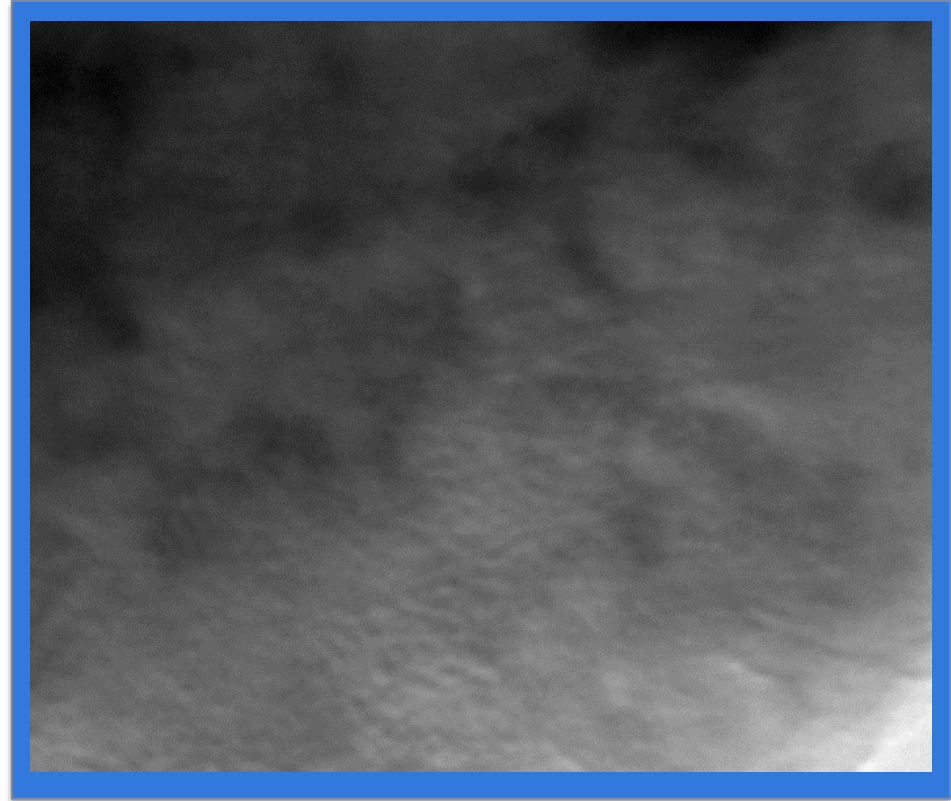
In-situ He implantation @ 310°C

- ❖ Each frame = 1 min of irradiation
- ❖ Because the cavities are difficult to see in powders, I paused the video at a few points to show overfocus images
- ❖ Electron beam on for most of experiment
- ❖ Bubbles formed after ~13 min (1.5×10^{17} He/cm²)

After Irradiation



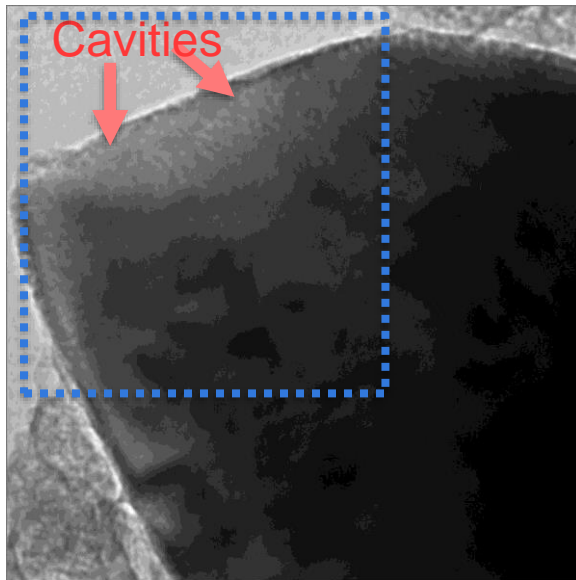
In-situ Video



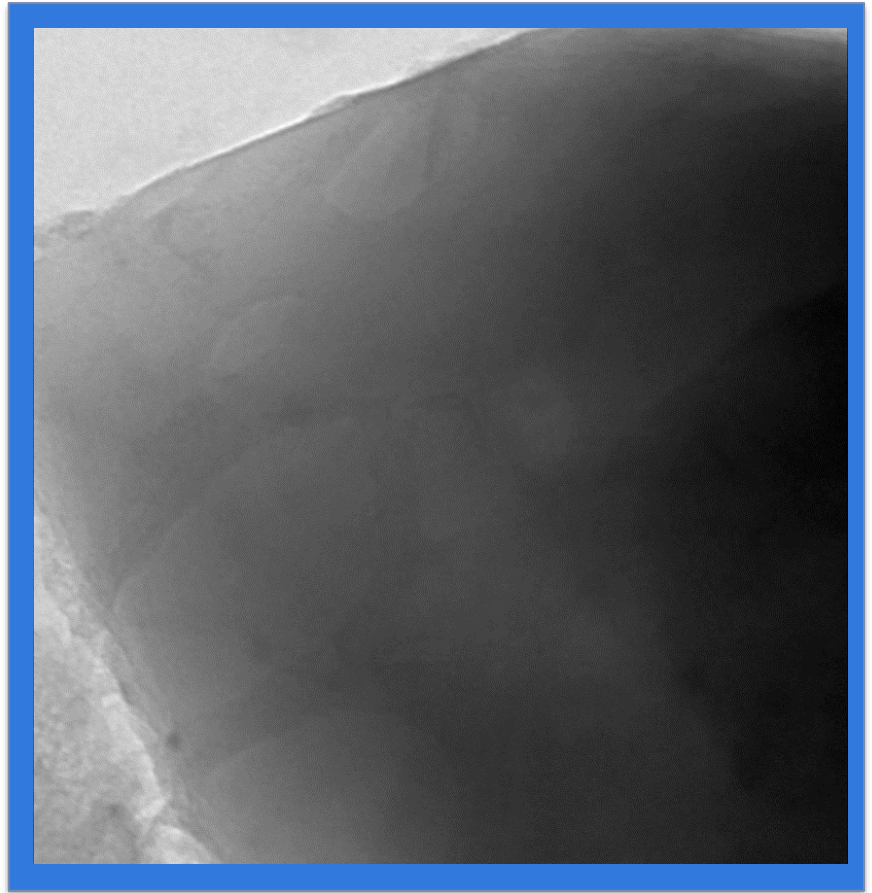
In-situ He + D irradiation @ 310°C

- ❖ Each frame = 5 min of irradiation
- ❖ All underfocus images
- ❖ Electron beam was off except for imaging
- ❖ Bubbles formed after ~60 min (1.7×10^{17} He/cm², 3.4×10^{17} D/cm²)

After Irradiation



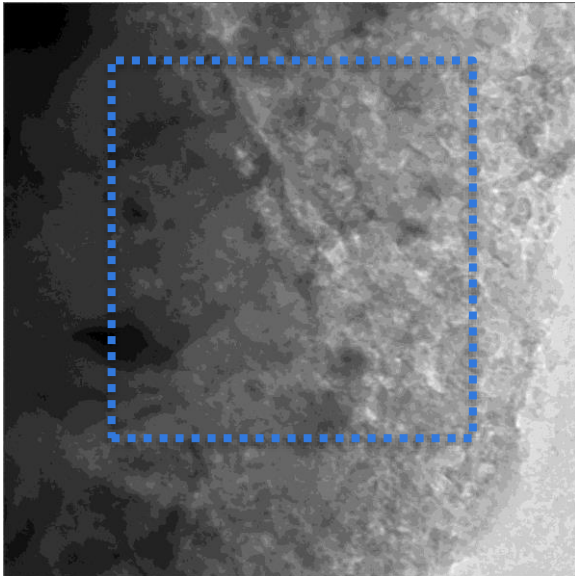
In-situ Video



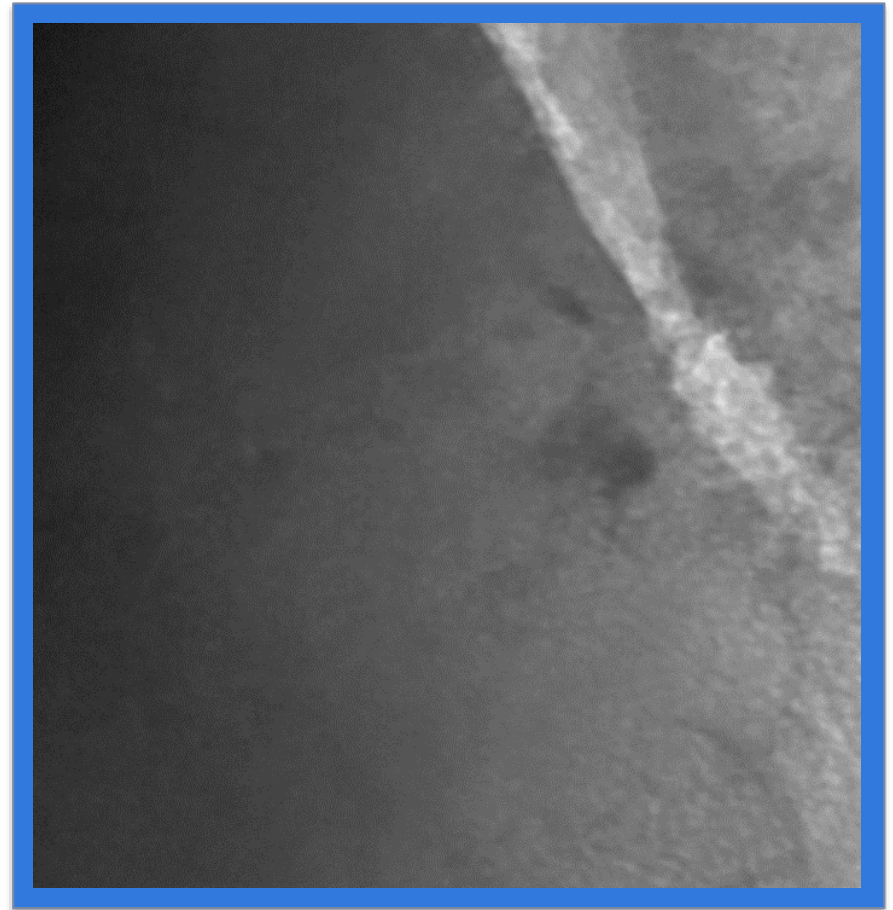
In-situ He + D + Au @ 310°C

- ❖ Each frame = 5 min of irradiation
- ❖ Pre-existing voids could have an effect on this final microstructure
- ❖ Electron beam was on for most of the experiment

After Irradiation



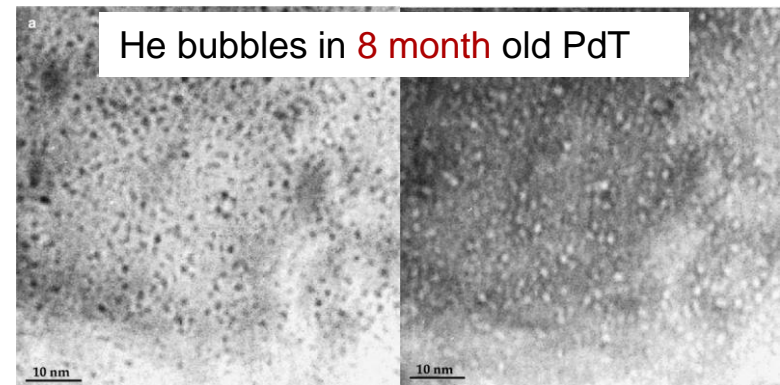
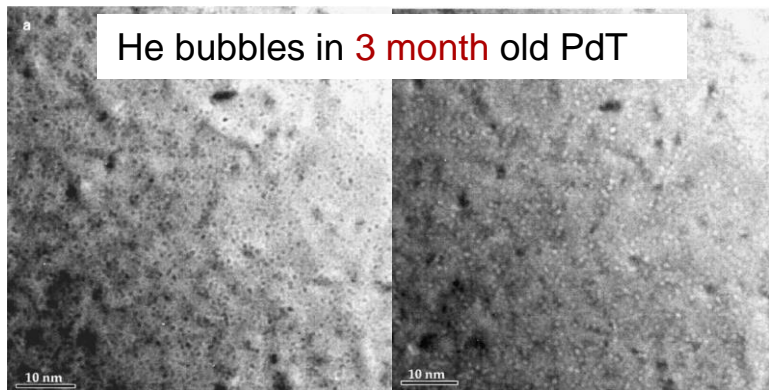
In-situ Video



Helium Bubble Nucleation and Growth in Palladium

Background

- Palladium is being considered for solid-state tritium storage
 - Helium accumulation
 - Due to rapid ^3He production in tritiated materials, He bubble formation will eventually lead to blister formation.
 - Blisters bursting the surface release ^3He and ^3H from the material.
 - Previous work:
 - He implantation to high doses, followed by thermal release measurements and SEM images of blisters.
 - Large database of microscopy and release measurements on aged PdT.
- ❖ Bubble nucleation mechanisms in PdT are currently unknown. Necessary for predictive aging models.



Irradiation temperatures

Diffusion mechanisms as a function of irradiation temperature:

1. Athermal displacement mixing mechanism. He diffusion is due to direct displacement. Dominant below annealing stage III where vacancies are immobile ($T < 0.2 T_m$).
2. Replacement mechanism. A He atom diffuses interstitially between its athermal replacement from a vacancy by a SIA and its re-trapping by another vacancy ($0.2 T_m < T < 0.5 T_m$). *Self interstitials mobile?*
3. Radiation enhanced vacancy mechanism. Dominates the replacement mechanism at temperatures above $0.5 T_m$. Cooperative with (1), so the fastest mechanism is the dominant one.

$$T_m = 1,555^\circ\text{C}$$

25 &
250°C

400°C

Too much grain
dropout in the
thin foil to
operate at
above ~500°C

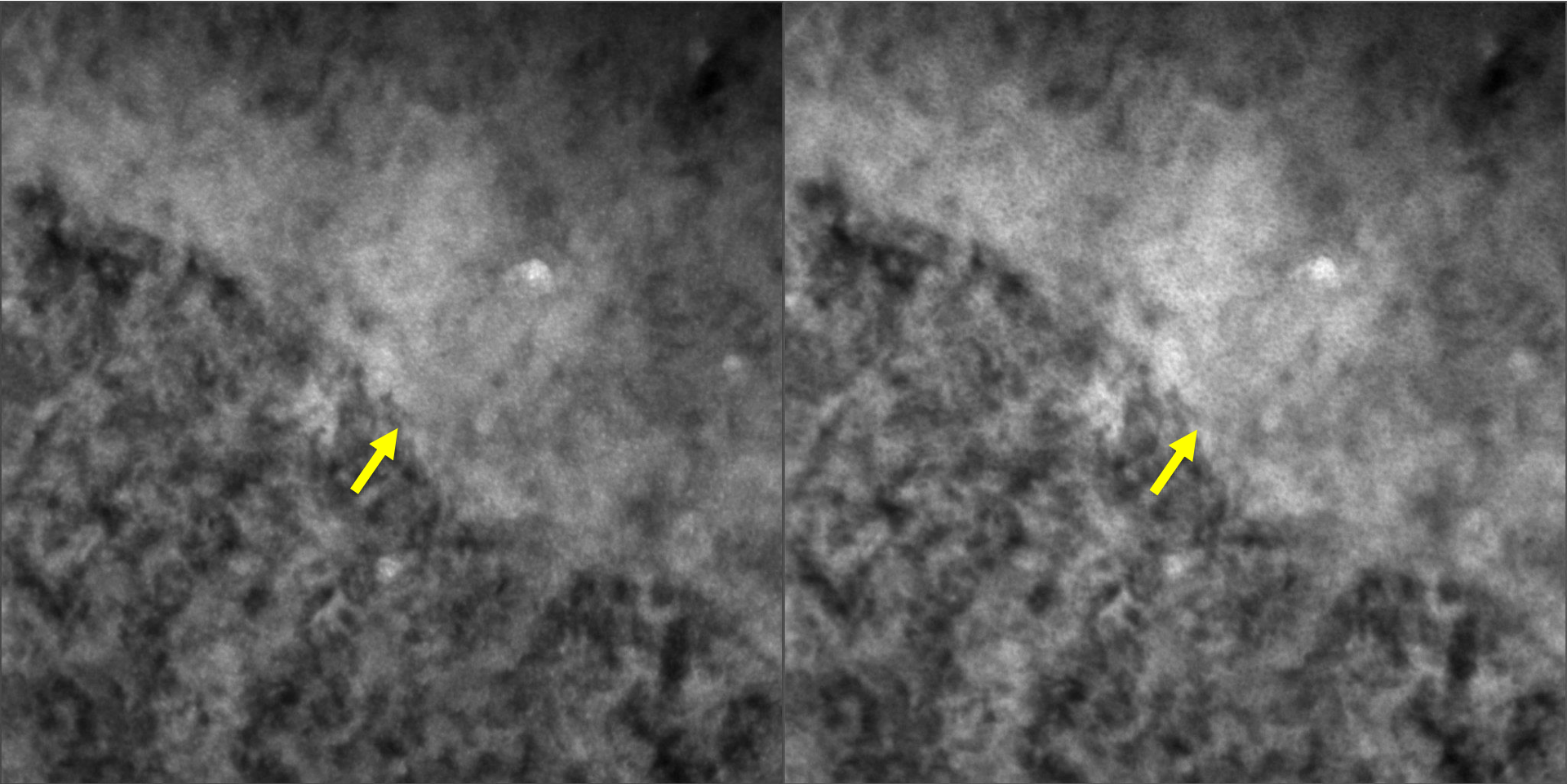
In the absence of radiation damage (e.g. tritide): He diffuses interstitially until the thermal vacancy concentration becomes significant at $\sim 0.5 T_m$.

Trinkaas and Singh, JNM 323 (2003) 229-242

Uniform distribution of bubbles was observed at room temperature

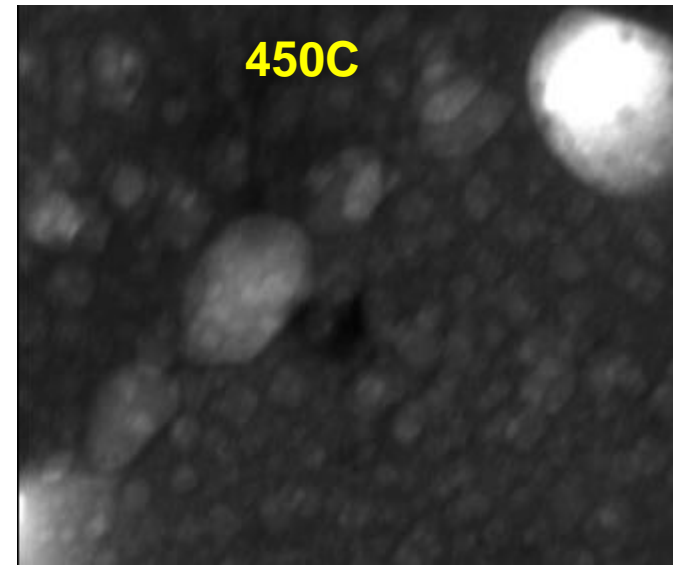
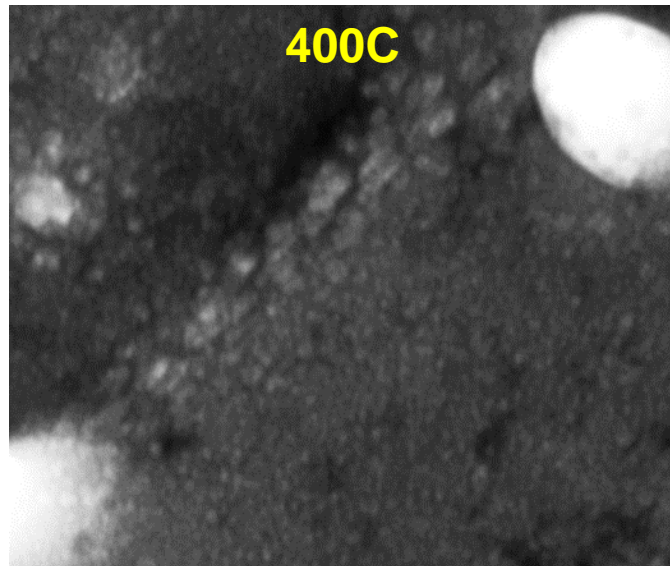
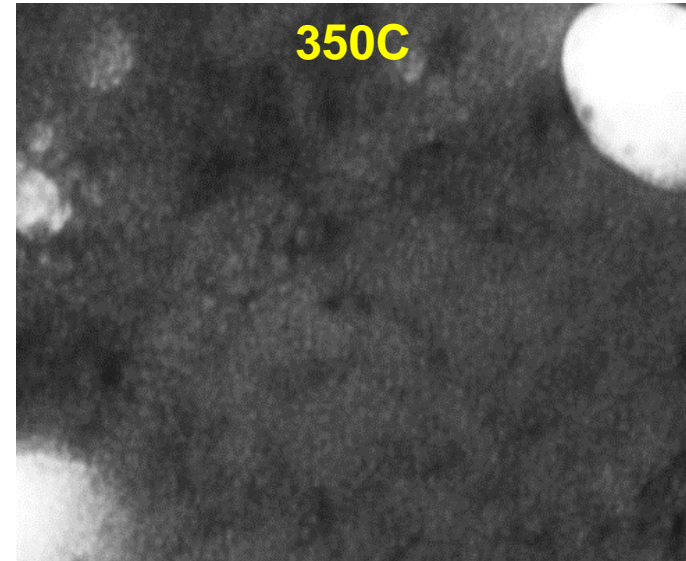
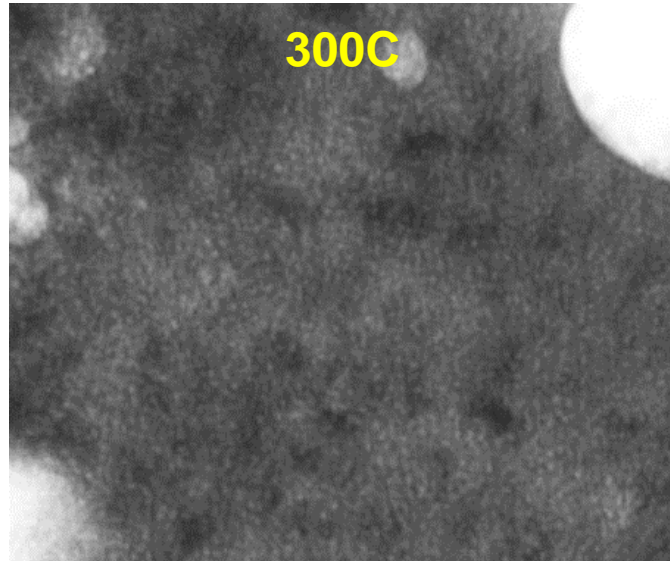
-230 nm defocus

+230 nm defocus



- ❖ Helium bubbles are spaced approximately nm apart.
- ❖ Bubbles did not show preferential nucleation at boundaries

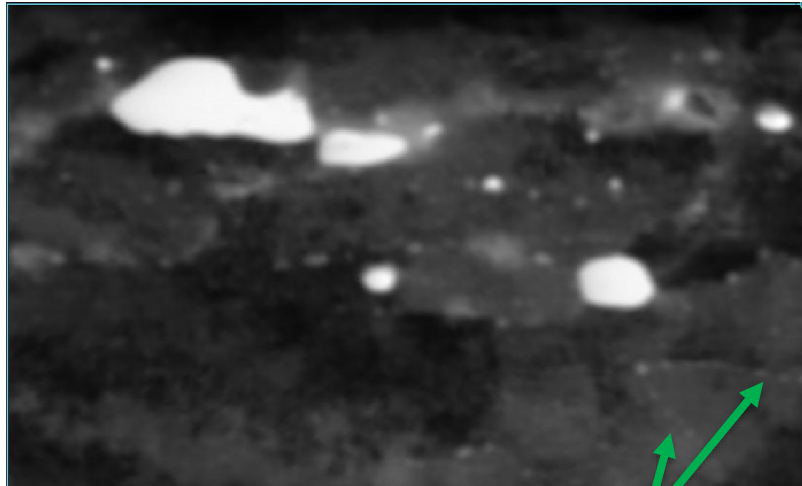
Bubble migration and growth mechanisms were observed during annealing



Orientation Mapping of Annealed Sample

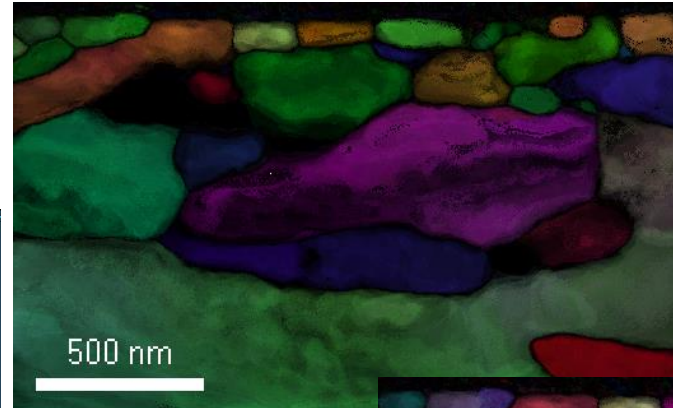
Nanomegas precession electron diffraction

Series Area

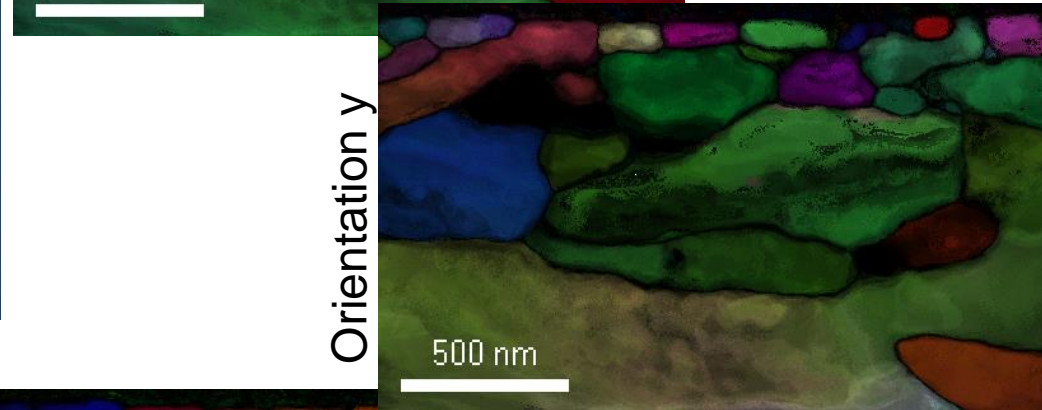


Bubbles along boundary

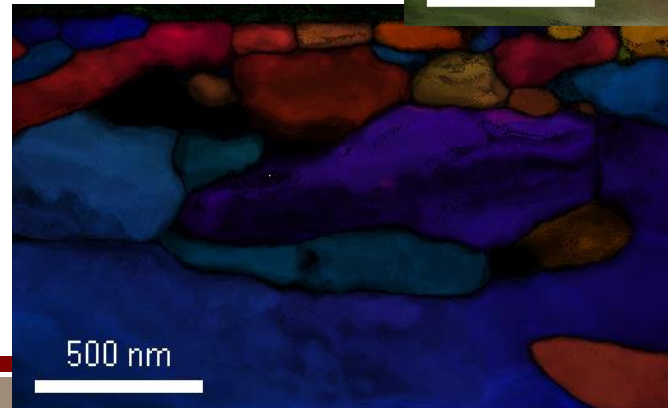
Data can be used to characterize grain boundaries where bubbles nucleated



Orientation x



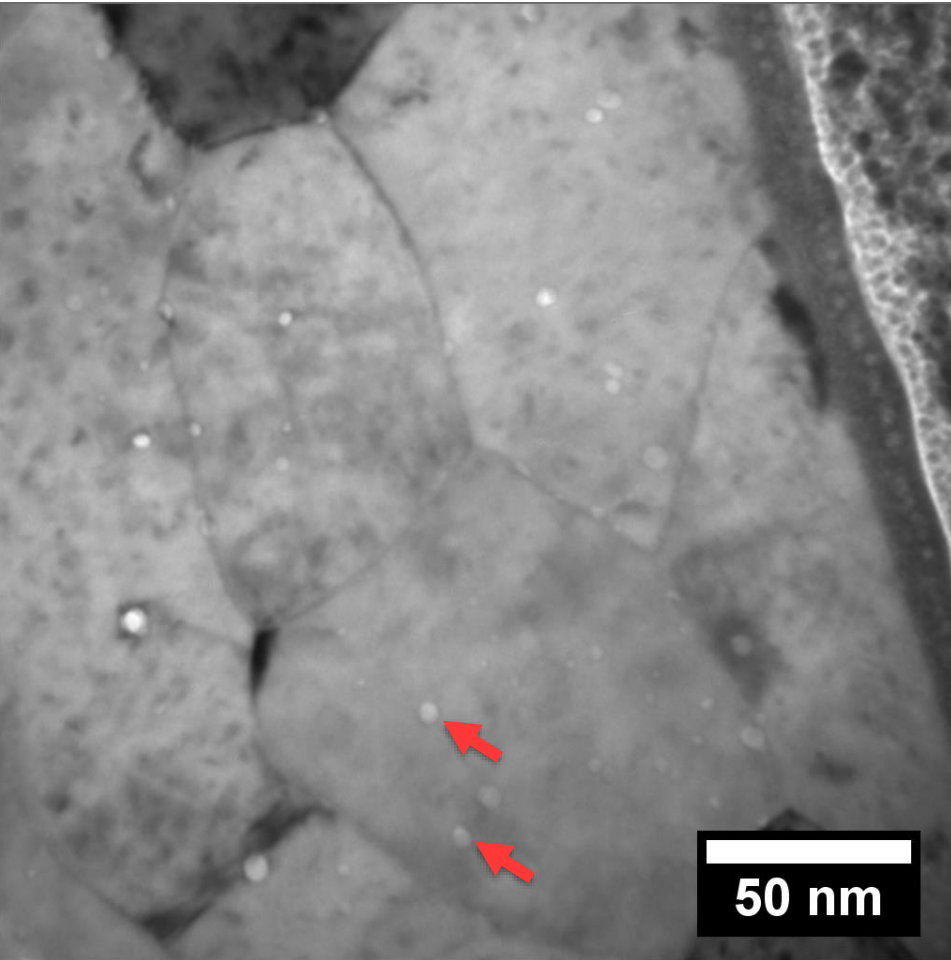
Orientation y



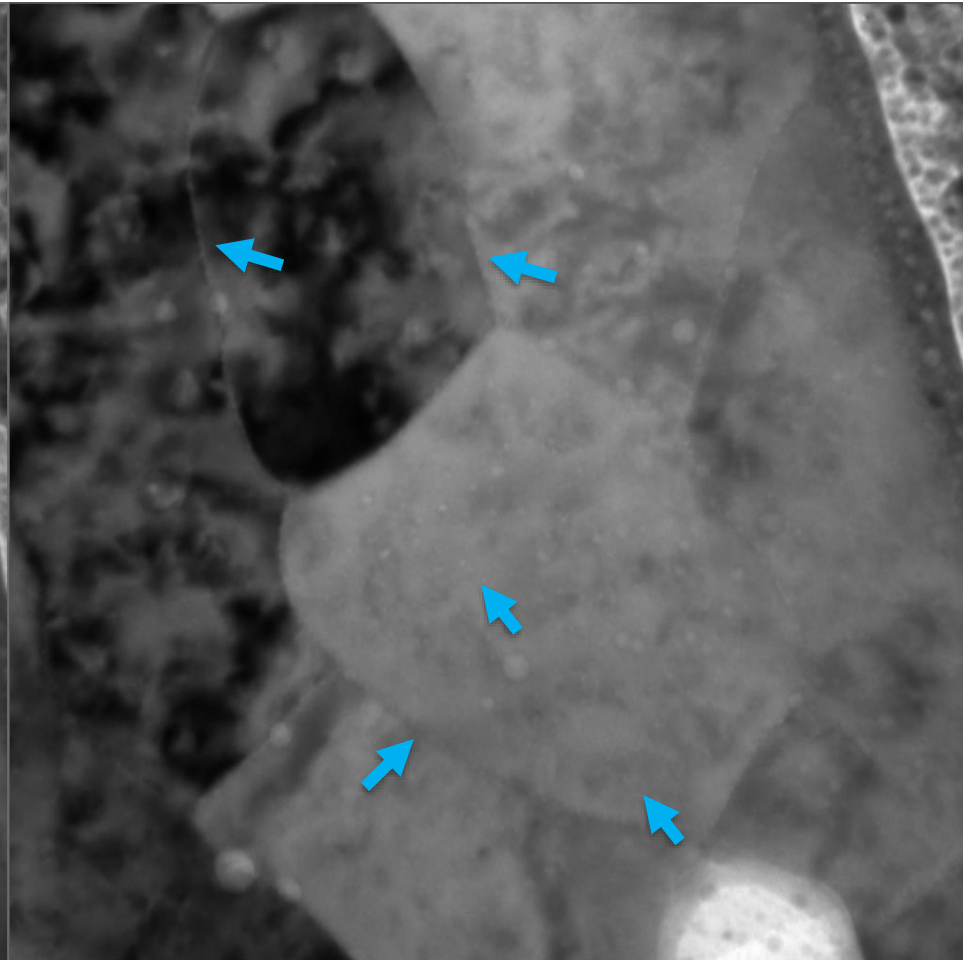
Orientation z

250°C: before and after, Spot 1

Before



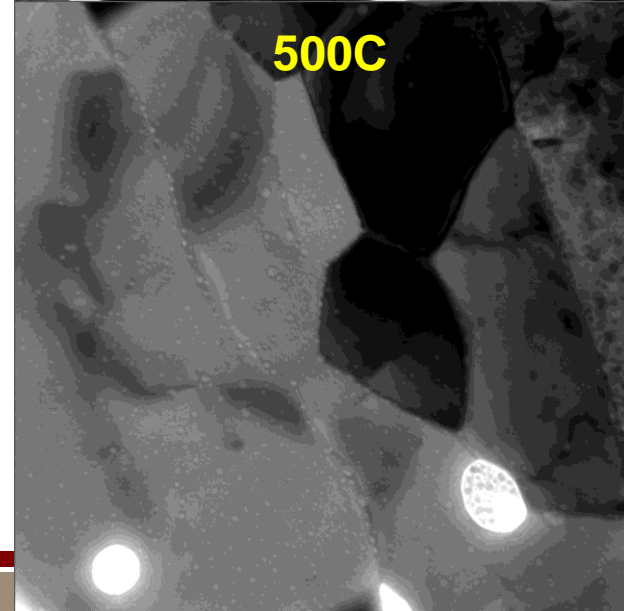
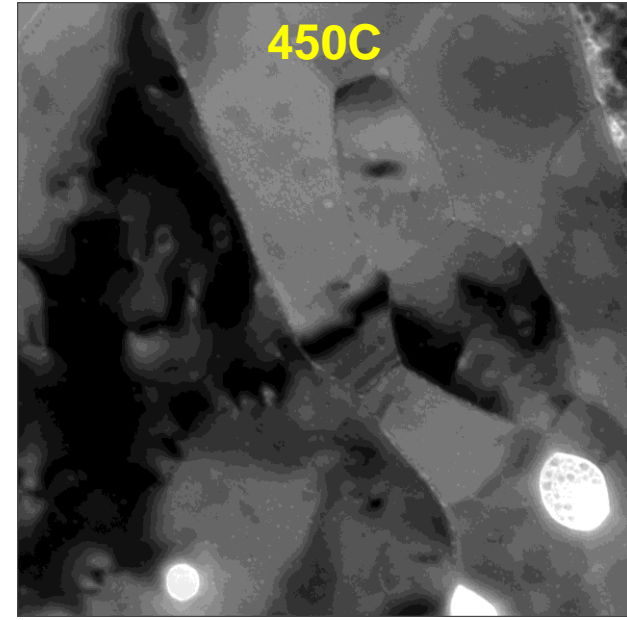
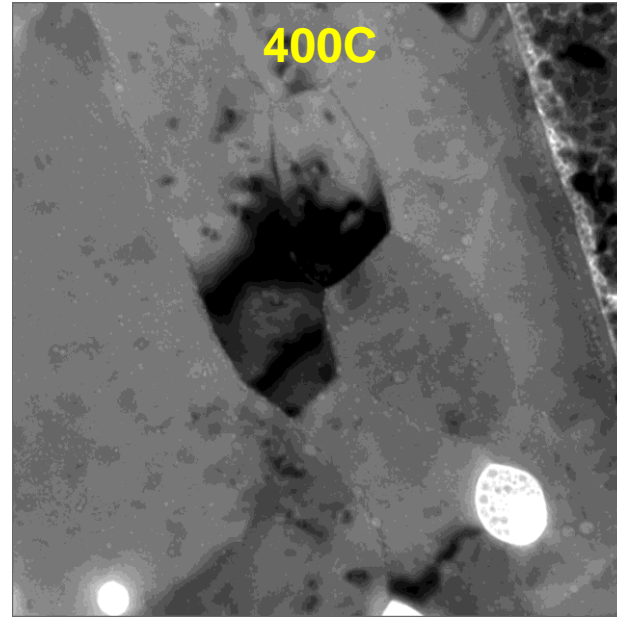
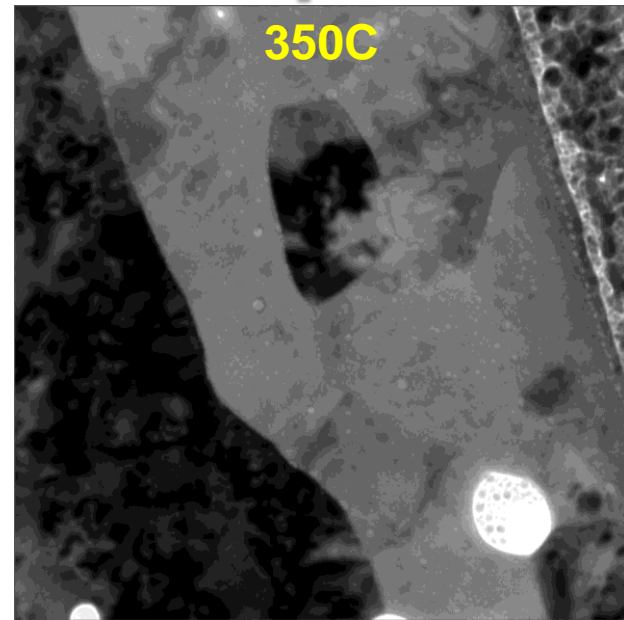
After



Pre-existing voids marked with red arrows either disappeared or shrunk after in-situ implantation

Cavities formed along boundaries and inside the grains during in-situ irradiation (marked by arrows).

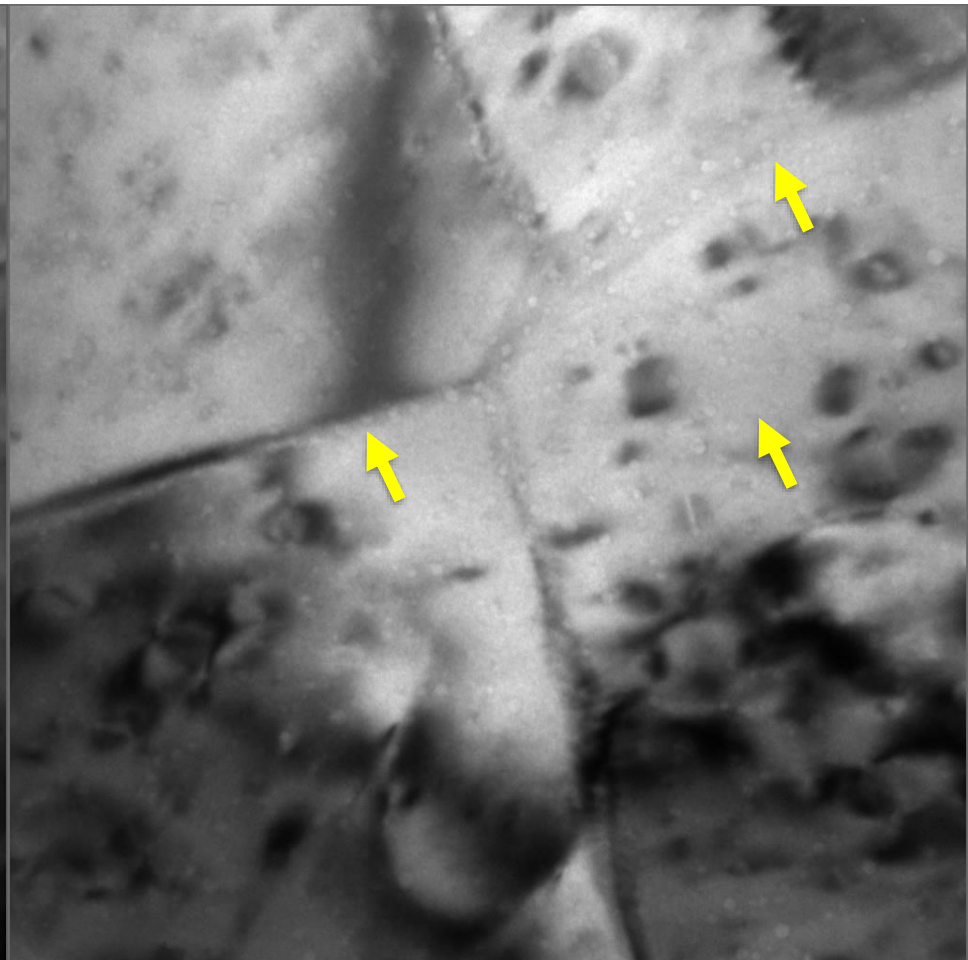
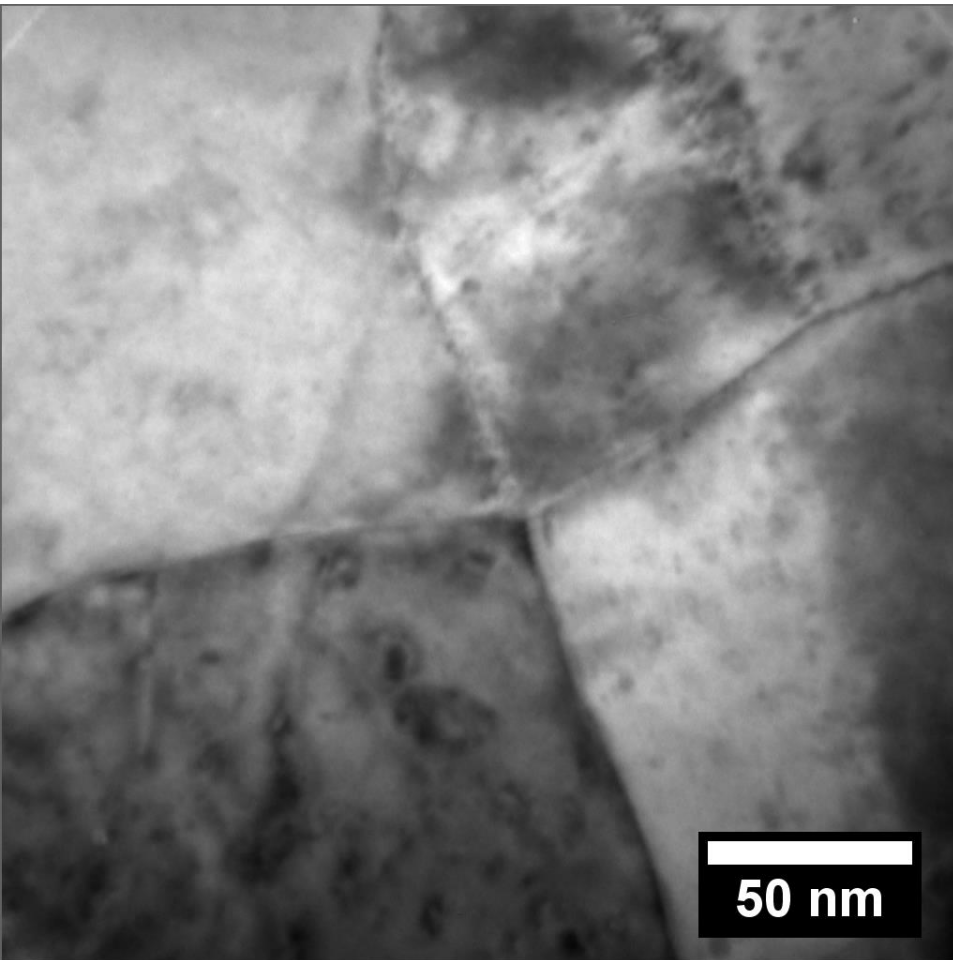
No observable bubble growth until 500C after 250C implantation



400°C: before and after, Spot 2

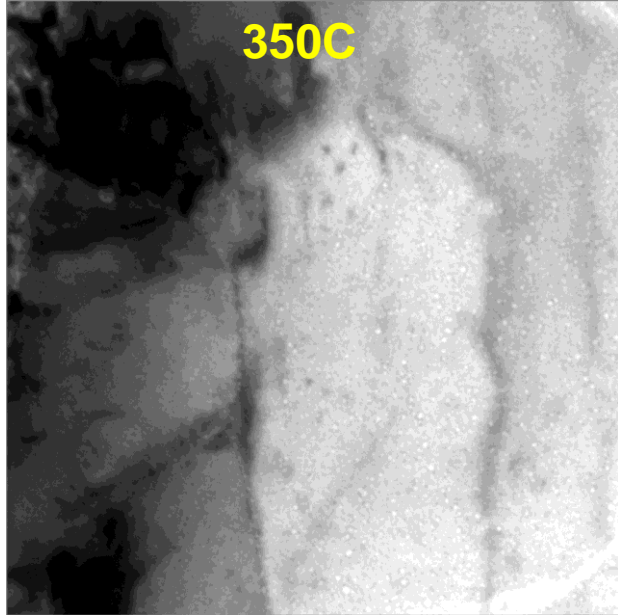
Before

After

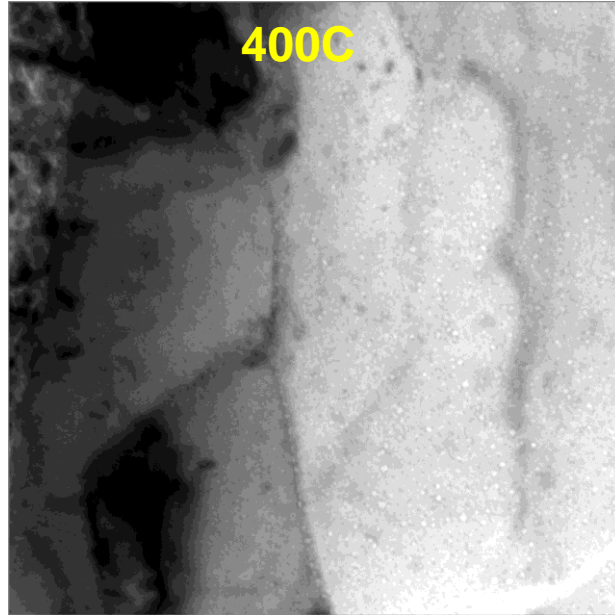


Images after annealing for 10 min @ each temp

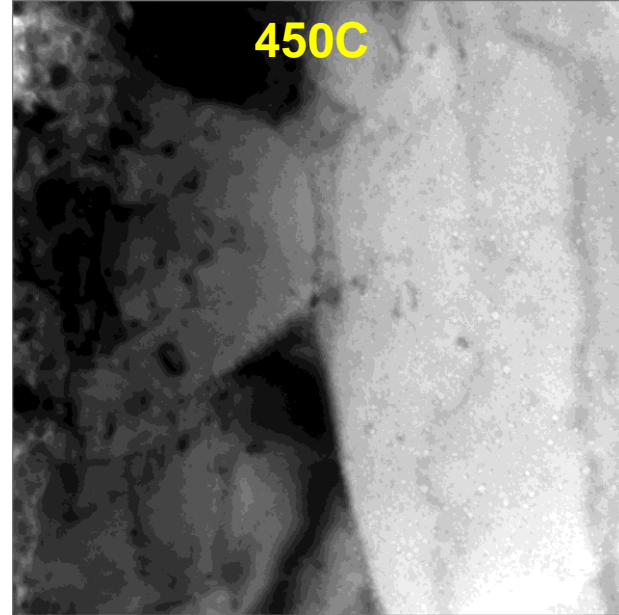
350C



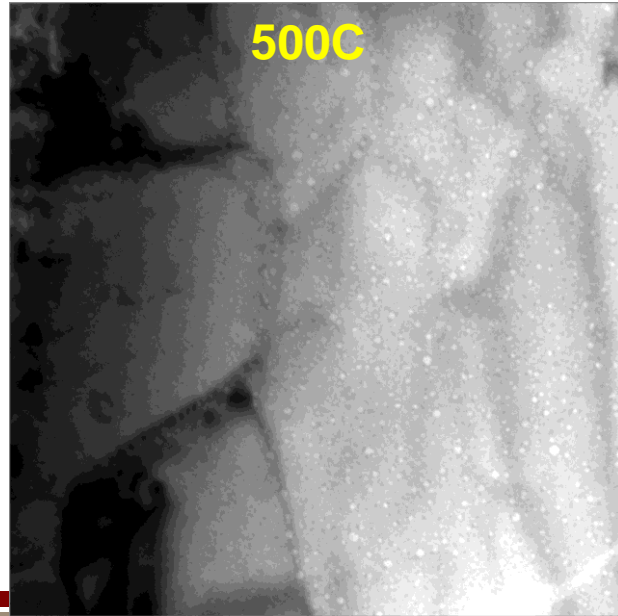
400C



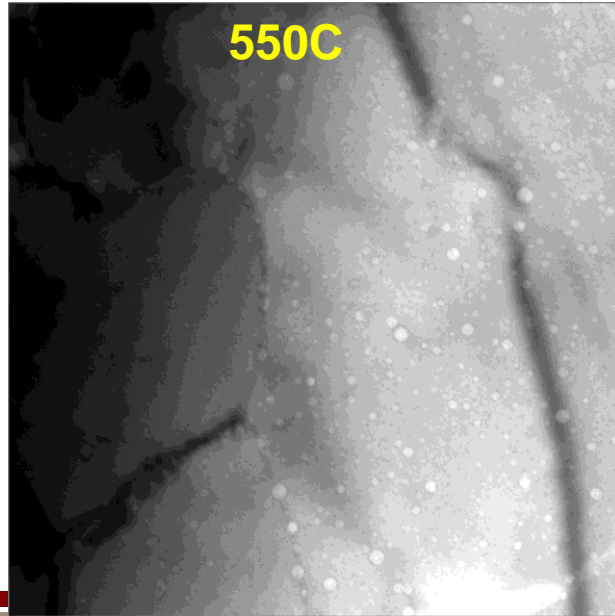
450C



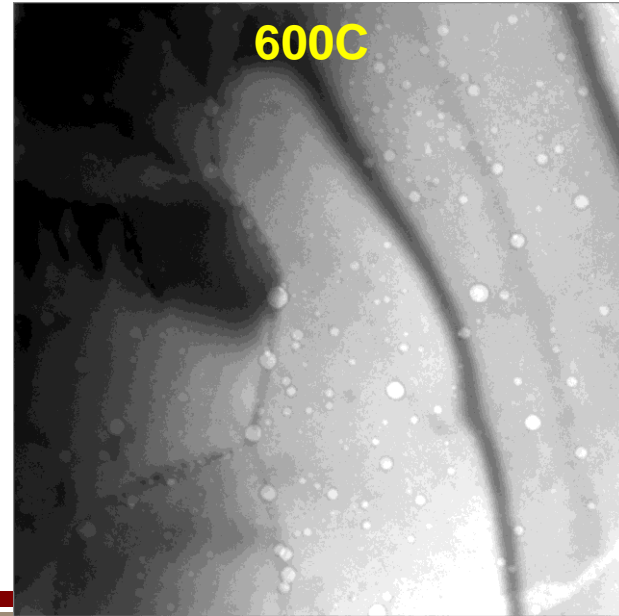
500C



550C



600C

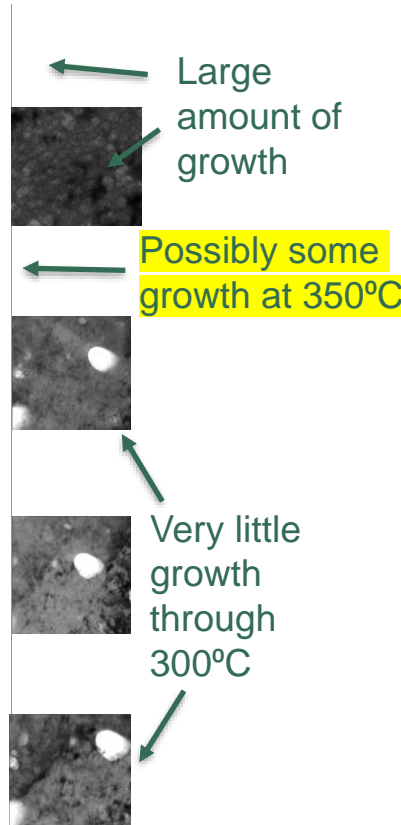
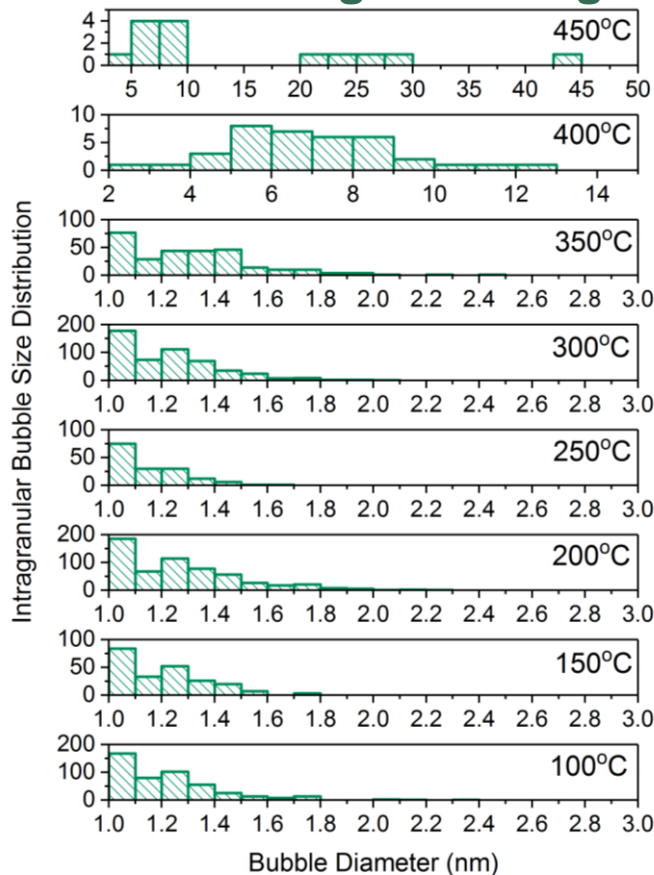


Bubble nucleation and growth summary

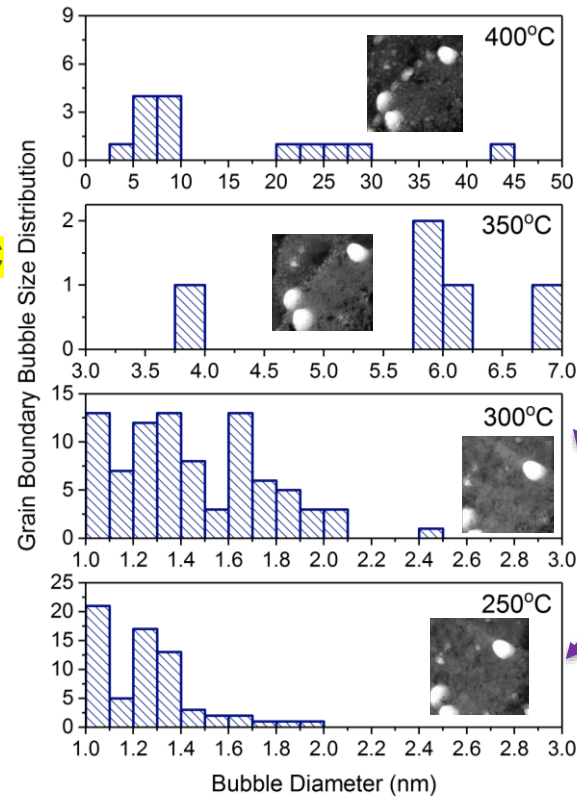
Behavior during implantation

- Bubbles did not nucleate at boundaries at room temperature
- Homogeneous nucleation. Bubbles were all approximately the same size.
- Bubbles nucleated ~ ____ nm apart

Intragranular bubble growth during annealing:



Grain boundary growth initiated at 250°C:



Blisters formed at 450°C and burst

Growth occurred at GBs but not inside grains

Collaborators

❖ Pyrochlore work:

- Maulik Patel (UTK, Liverpool)
- Jeffery Aguiar (NREL, INL)
- Miguel Crespillo & Haizhou Xue (UTK)
- Yongqiang Wong (LANL)
- Xunxiang Xu (ORNL) & Brian Wirth (UTK, ORNL)
- Bill Weber & Yanwen Zhang (UTK, ORNL)
- This project was funded by Nuclear Energy University Programs award number 12-3528



❖ LiAlO₂ work:

- Dave Senior (PNNL)
- Brittany Muntifering (SNL)
- Khalid Hattar (SNL)

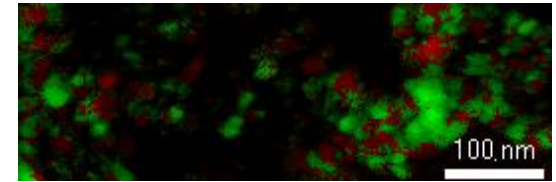
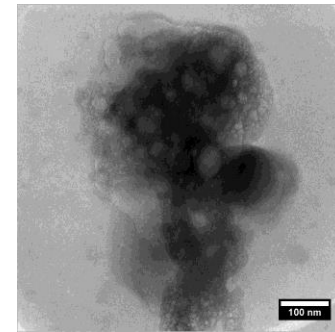
❖ Palladium work:

- Dave Robinson (SNL-CA)
- Joshua Sugar (SNL-CA)
- Brittany Muntifering (SNL)
- Khalid Hattar (SNL)



Technical Qualifications

- ❖ Transmission Electron Microscopy (TEM)
 - Conventional TEM imaging in Zeiss, JEOL, and FEI microscopes
 - In-situ ion irradiation and gas implantation
 - In-situ annealing with Gatan and Hummingbird stages
 - In-situ gas cell (Protochips)
 - In-situ microfluidic cell (Protochips)
 - Nanomegas grain orientation mapping
- ❖ Scanning Electron Microscopy (SEM) and Energy Dispersive Spectroscopy (EDS)
 - Mainly Zeiss microscopes
- ❖ Additional characterization techniques:
 - Powder X-ray Diffraction (XRD) and indexing with Jade or HighScore Plus software
 - Grazing-incidence X-ray diffraction (GIXRD)
 - High resolution X-ray diffraction and reciprocal space mapping
 - Experience analyzing thermal desorption spectroscopy (TDS) data
 - Experience analyzing data from various ion beam analysis techniques
- ❖ Experience working with large teams of experimentalists and modelers on multi-institutional projects (e.g. with PNNL, ORNL, SNL-CA)
- ❖ Experience working in the Nuclear Weapons complex
- ❖ Experience working in radiation facilities. Currently work in a tritium envelope with radioactive neutron generator components.



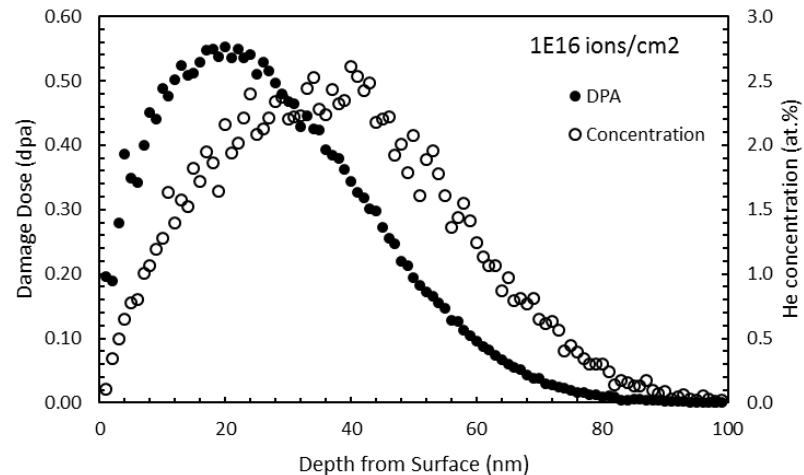
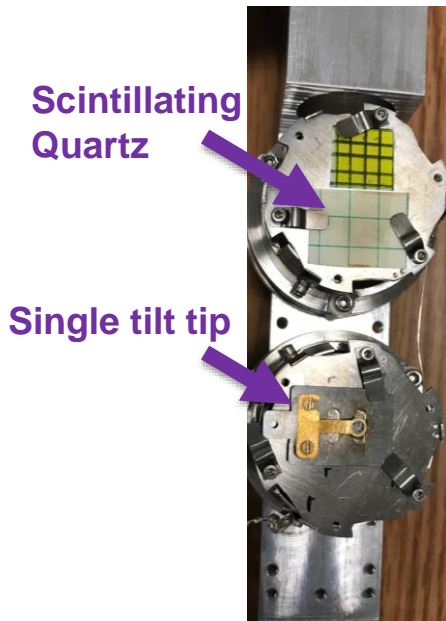
Backup Slides

Ex-situ He Implantation and Annealing

Procedure:

1. Put FIB liftout in JEOL single tilt stage and imaged.
2. Aligned 10 keV He beam from the Colutron inside the implantation chamber using quartz.
3. Mount single tilt stage tip inside implantation chamber using clips.
4. Implant the sample with He at room temperature.
5. Image the sample after each implantation step inside the TEM until bubbles form.
6. Transfer sample to Gatan heating stage and anneal.

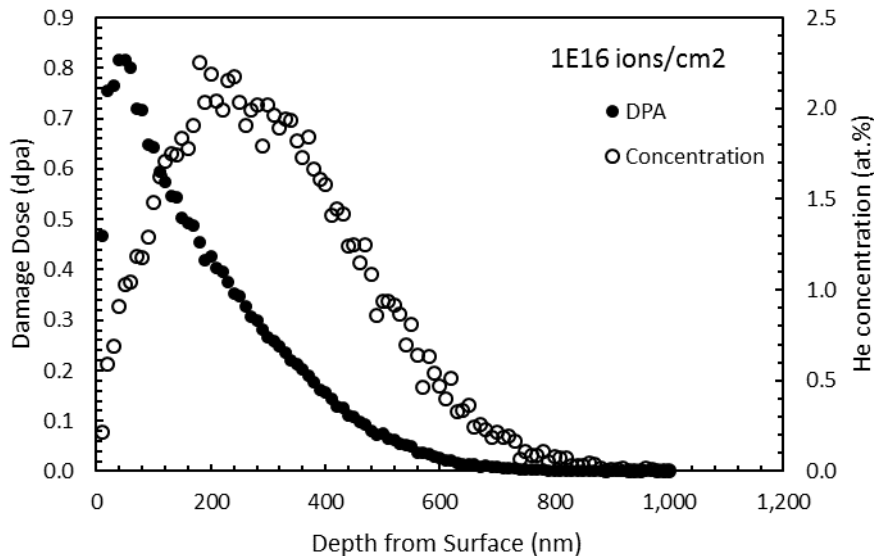
He beam



In-situ He Implantation and Annealing

Procedure:

1. Aligned 10 keV He beam from the Colutron inside the TEM using quartz and JEOL single tilt stage.
2. Imaged samples in Gatan heating stage at 0° tilt and 25°C
3. Tilted to 30° in +x for the implantation. Heated the sample to desired temperature.
4. After implantation, tilted back to 0° tilt for post-characterization at room temperature, followed by annealing.



Fluences cannot be accurately determined during this experiment. The **depth profile** calculated by SRIM (left) *is* accurate, and is scaled in the vertical direction with change in fluence.